

Supporting Information

Unveiling the Mechanism of the Photocatalytic Reduction of CO₂ to Formate Promoted by Porphyrinic Zr-Based Metal-Organic Frameworks.

Youven Benseghir,^{a,b,‡} Albert Solé-Daura,^{a,‡} Daniel R. Cairnie,^{c,‡} Amanda L. Robinson,^a Mathis Duguet,^{a,b} Pierre Mialane,^{*,b} Priyanka Gairola,^b Maria Gomez-Mingot,^a Marc Fontecave,^a Diana Iovan,^c Brittany Bonnett,^c Amanda J. Morris,^{*,c} Anne Dolbecq^b and Caroline Mellot-Draznieks^{*,a}

^a Laboratoire de Chimie des Processus Biologiques, UMR CNRS 8229, Collège de France, Sorbonne Université, PSL Research University, 11 Place Marcelin Berthelot, 75231 Paris Cedex 05, France

^b Université Paris-Saclay, UVSQ, CNRS UMR 8180, Institut Lavoisier de Versailles

^c Department of Chemistry, Virginia Tech, Blacksburg, Virginia, 24060, USA.

E-mail:

pierre.mialane@uvsq.fr

ajmorris@vt.edu

caroline.mellot-draznieks@college-de-france.fr

Table of Contents

1. Materials, experimental and physical methods	S5
Figure S1. Experimental X-ray powder patterns of MOF-545(TM) a) used in photocatalytic measurements and b) in photophysical measurements; c) SEM image of MOF-545 used for photophysical measurements.	S9
Figure S2. FT-IR spectra of MOF-545(TM).	S11
Figure S3. UV-visible absorption spectra of MOF-545(TM).	S12
Figure S4. TGA curves of NanoMOF-545 and NanoMOF-545(Fe).	S13
Figure S5. BET N ₂ adsorption/desorption isotherms of MOF-545, MOF-545(Fe), NanoMOF-545 and NanoMOF-545(Fe).	S13
Figure S6. XPS spectra recorded on NanoMOF-545(Fe).	S14
Figure S7. Time evolution of the visible-light-driven formate production for NanoMOF-545(Fe) and recyclability experiments for NanoMOF(Fe).	S14
Figure S8: PXRD pattern of MOF-545, NanoMOF-545(Fe) before and after catalysis after 4h catalytic run.	S15
Table S1: Photocatalytic reduction of CO ₂ using MOF-545(TM).	S15
Table S2. Comparison of HCOO ⁻ production from photocatalytic CO ₂ reduction by MOF-based photocatalytic systems.	S16
2. Analysis of the evolution of UV spectra with time / photophysical measurements	S17
Table S3. Photophysical data of MOF-545 and MOF-545(Zn) suspensions.	S18
Table S4. Photophysical data of TCPP and (Zn)TCPP in Ar-purged DMF solutions.	S18
Figure S9. Steady-state electronic absorption spectra of H ₂ TCPP in 10:1 (v/v) DMF/TEOA.	S19
Figure S10. Steady-state excitation spectra of MOF-545 and MOF-545(Zn) in DMF.	S19
Figure S11. Steady-state emission spectra of TCPP and (Zn)TCPP in DMF.	S20
Figure S12. Emission decay trace of TCPP in DMF.	S20
Figure S13. Emission decay trace of (Zn)TCPP in DMF.	S20
Figure S14. Transient absorption time-map of freebase TCPP in DMF.	S21
Figure S15. Excited-state absorption decay trace of freebase TCPP in DMF measured at 450 nm.	S21
Figure S16. Ground-state bleach recovery trace of freebase TCPP in DMF measured at 419 nm.	S21
Figure S17. Transient absorption time-map of freebase TCPP in a solution of PEGNH ₂ in DMF.	S22

Figure S18. Excited-state absorption decay trace of freebase TCPP in a solution of PEGNH ₂ in DMF measured at 460 nm.	S22
Figure S19. Ground-state bleach recovery trace of freebase TCPP in a solution of PEGNH ₂ in DMF measured at 419 nm.	S22
Figure S20. Transient absorption time-map of (Zn)TCPP in DMF.	S23
Figure S21. Excited-state absorption decay trace of (Zn)TCPP in DMF measured at 460 nm.	S23
Figure S22. Ground-state bleach recovery trace of (Zn)TCPP in DMF measured at 427 nm.	S23
Figure S23. Transient absorption time-map of (Zn)TCPP in a solution of PEGNH ₂ in DMF.	S24
Figure S24. Excited-state absorption decay trace of (Zn)TCPP in a solution of PEGNH ₂ in DMF measured at 460 nm.	S24
Figure S25. Ground-state bleach recovery trace of (Zn)TCPP in a solution of PEGNH ₂ in DMF measured at 430 nm.	S24
Figure S26. Steady-state transient absorption spectrum of MOF-545 in a solution of PEGNH ₂ in DMF.	S25
Figure S27. Excited-state absorption decay trace of MOF-545 in a solution of PEGNH ₂ in DMF.	S25
Figure S28. Ground-state bleach recovery trace of MOF-545 in a solution of PEGNH ₂ in DMF.	S25
Figure S29. Steady-state electronic absorption spectra of MOF-545 in a solution of PEGNH ₂ in DMF.	S26
Figure S30. Steady-state electronic absorption spectra of MOF-545(Zn) in a solution of PEGNH ₂ in DMF.	S26
3. Computational results	S27
Figure S31. Density of States calculated for the Zr ₆ -oxo cluster, the MOF-545 and a series of MOF-545(TM).	S27
Figure S32. UV-Vis spectra obtained by means of TD-DFT (ω B97X-D/DZP level).	S28
Table S5. Analysis of the 6 first excited states obtained from time dependent DFT calculations for the H ₂ TCPP-Zr ₆ system represented in Figure S32.	S29
Figure S33. Simulated absorption spectrum for the one-electron reduced Zn ^{II} -TCPP ^{•-} -Zr ₆ model.	S29
Figure S34. Optimized geometry for TS ₂₋₃ and representation of the spin density distribution in the structure of TS ₂₋₃ .	S30
Figure S35. Optimized geometry for species 3 and representation of the spin density distribution in the structure of 3.	S30
Figure S36. DFT-optimized structures of the 2-TEOA [•] non-covalent adduct (top) and TS ₂₋₄ .	S31
Figure S37. Optimized structure of the product generated after TS ₂₋₄ , corresponding to the hydrogen-bonded adduct between 4 and the neutral aldehyde radical derived from TEOA.	S31
Figure S38. Geometry, energy and spin-density evolution along the geometry optimization from TS ₂₋₄ to products.	S32

Scheme S1. Proposed pathway and transient intermediates involved in the formal hydride-transfer process from TEOA [•] to CO ₂ .	S32
Figure S39. Hydrogenation of CO ₂ promoted by TEOA [•] <i>without</i> the assistance of a Zr ^{IV} center as Lewis acid.	S33
Figure S40. Free energy cost (kcal·mol ⁻¹) associated to the release of the HCOOH product from the Zr-oxo cluster.	S33
Scheme S2. Possible termination routes after the CO ₂ reduction step. Relative Gibbs free energies and reaction energies are given in kcal·mol ⁻¹ .	S34
4. NMR and mass spectrometry experiments	S34
Figure S41. ¹ H NMR spectrum of the reaction mixture after the catalysis.	S34
Figure S42. HRMS spectrum of the reaction mixture after 4h of photocatalytic experiments with NanoMOF-545(Fe).	S35
Figure S43. Expected HRMS spectrum for C ₆ H ₁₃ NO ₃ and experimental HRMS spectrum.	S35
Figure S44. Expected HRMS spectrum for C ₆ H ₁₁ NO ₃ and experimental HRMS spectrum.	S35
Figure S45. Expected HRMS spectrum for C ₆ H ₉ NO ₃ and experimental HRMS spectrum	S36
5. Additional computational results	
Figure S46. Calculated Gibbs free-energy profile (kcal·mol ⁻¹) for the reduction of CO ₂ from species 4.	S36
6. Use of DMPO radical scavenger in photocatalytic reduction of CO₂	S37
Figure S47. Use of DMPO radical scavenging in the photocatalytic reduction of CO ₂ with MOF-545(Fe).	S37
7. UV-Vis Spectral Titrations of FeTCPPCl and ZnTCPP	S37
Figure S48. Steady-state electronic absorption spectra of 28 μM ZnTCPP in DMF with increasing equivalents of TEOA added.	S38
Figure S49. Absorbance change (OD _[TEOA] – OD _{initial}) of ZnTCPP with increasing [TEOA].	S38
Figure S50. Steady-state electronic absorption spectra of Fe ^{III} TCPPCl with increasing equivalent of TEOA added.	S39
Figure S51. Absorbance change (OD _[TEOA] – OD _{initial}) of Fe ^{III} TCPPCl with increasing [TEOA].	S39
8. References	S40
9. Optimized Cartesian Coordinates (Å) and Gibbs Free Energies (a.u.) for the most representative structures obtained at the ωB97X-D level	S41

1. Materials, experimental and physical methods.

The solvents dimethylformamide (DMF, >99.8 %) and acetonitrile (CH_3CN , >99 %) were supplied by Fischer Scientific. Triethanolamine (TEOA, >99 %) was purchased from Sigma-Aldrich. The buffer 2-[4-(2-hydroxyethyl)piperazin-1-yl]ethane-1-sulfonic acid (HEPES, >99.5 %) and salt (Na-HEPES, 99 %), were purchased from Sigma-Aldrich and ACROS Organics, respectively. Poly(ethylene glycol) bis(3-aminopropyl)-terminated ($\text{PEG}(\text{NH}_2)_2$, $M_n \sim 1500$) was purchased from Sigma-Aldrich. The synthetic modulators 1,2-dichloroacetic acid and 1,2-difluoroacetic acid were purchased from Sigma-Aldrich. $\text{FeCl}_2 \cdot 6\text{H}_2\text{O}$, $\text{MnCl}_2 \cdot 4\text{H}_2\text{O}$, ZnCl_2 , $\text{CoCl}_2 \cdot 6\text{H}_2\text{O}$, $\text{CuCl}_2 \cdot 6\text{H}_2\text{O}$ and $\text{ZrOCl}_2 \cdot 8\text{H}_2\text{O}$ were purchased from Alfa Aesar. $\text{Zn}(\text{NO}_3)_2 \cdot 6\text{H}_2\text{O}$ was purchased from Sigma-Aldrich. Methyl-p-formylbenzoate, pyrrole and propionic acid were purchased from TCI Chemicals. All compounds were used without further purification.

Linkers Synthesis. TCPPOMe, (M)TCPPOMe, H_2TCPP and (M)TCPP (M = Fe, Cu, Co, Mn, Zn) were synthesized as described by Feng *et al.*¹

MOF-545(M) (M = Cu, Co, Mn, Zn) synthesis (for characterization and photocatalytic experiments). MOF-545(M) was synthesized by adapting the procedure adopted by Paille *et al.* for the synthesis of the free base MOF-545.² Briefly, 275 mg of $\text{ZrOCl}_2 \cdot 8\text{H}_2\text{O}$, 60 mg of (M)TCPP and 2 mL of 1,2-dichloroacetic acid were dissolved in 80 mL of DMF. The mixture was heated at 130 °C overnight. After cooling to room temperature, the MOF powder was collected by centrifugation. The MOF was then heated at 130 °C for two hours in a 10 mL DMF / 1 mL 1M HCl mixture. After centrifugation, the obtained material was rinsed twice with DMF and twice with acetone. Lastly, the powder was dispersed in 20 mL of acetone and stirred overnight. The final compound was collected by centrifugation, rinsed twice with acetone and then dried at 100 °C (m = 55-65 mg). EDX calcd. (exp.) : MOF-545(Cu) : Cu/Zr 0.33 (0.37), MOF-545(Co) : Co/Zr 0.33 (0.26), MOF-545(Mn) : Mn/Zr 0.33 (0.35) and MOF-545(Zn) : Zn/Zr 0.33 (0.34).

MOF-545(Fe) synthesis (for characterization and photocatalytic experiments). For the synthesis of MOF-545(Fe), we noticed that a lower (Fe)TCPP/Zr ratio was necessary to get a crystalline powder. Also, a higher volume of acidic solution was used to wash the MOF. 375 mg of $\text{ZrOCl}_2 \cdot 8\text{H}_2\text{O}$, 60 mg of (Fe)TCPP and 2 mL of 1,2-dichloroacetic acid were dissolved in 80 mL of DMF. After cooling to room temperature, the MOF powder was collected by centrifugation. The MOF was then heated at 130 °C for two hours in a 30 mL DMF / 3 mL 1M HCl mixture. After centrifugation, the obtained material was rinsed twice with DMF and twice with acetone. Lastly, the powder was dispersed in 20 mL of acetone and stirred overnight. The final compound was collected by centrifugation, rinsed twice with acetone and then dried at 100 °C (m = 60 mg). EDX calcd. (exp.) : Fe/Zr 0.33 (0.35).

MOF-545 synthesis (for photolysis and photophysical measurements). MOF-545 was prepared *via* solvothermal synthesis as described in a previous work.³ Zirconyl chloride octahydrate ($\text{ZrOCl}_2 \cdot 8\text{H}_2\text{O}$; 38 mg, 0.118 mmol) and *meso*-tetrakis(4-carboxyphenyl)porphyrin (TCPP; 7 mg, 0.00885 mmol) were combined with difluoroacetic acid (DFA; 0.226 mL, 3.59 mmol) modulator and DMF (16 mL) in a 6-dram scintillation vial, sonicated until fully dissolved, and heated in a 120 °C oven for 18 h. The resulting violet crystalline powder was isolated via centrifugation, washed three times with DMF and acetone, and dried in a 60 °C oven overnight.

MOF-545(Zn) post-synthetic metalation (for photolysis and photophysical measurements). MOF-545(Zn) was prepared by adding MOF-545 (15 mg, 5.77×10^{-3} mmol) and a ten-fold molar excess of $\text{Zn}(\text{NO}_3)_2 \cdot 6\text{H}_2\text{O}$ (17.2 mg, 0.057 mmol) to a 1-dram vial. The vial was then filled up with DMF (2 mL), sonicated for 1-2 min, and placed in a 60 °C oven for 18 – 20 h. The resulting green-yellow suspension was isolated via centrifugation, washed three times with DMF and acetone, and dried in a 60 °C oven overnight.

Note that the MOF-545 derivatives for photophysical measurements have been synthesized via slightly different protocols than those used for characterization and catalytic experiments. PXRD, BET and SEM investigations performed on the obtained materials are in full agreement with the expected ones.

Physical methods. Infrared (IR) spectra were recorded on a Nicolet 30 ATR 6700 FT spectrometer. Powder X-ray diffraction (PXRD) data were obtained on a Bruker D5000 diffractometer using Cu K- α radiation (1.54059 Å). Energy dispersive spectroscopy (EDS) measurements were performed on a JEOL JSM 5800LV apparatus. N_2 adsorption isotherms were obtained at 77 K using a BELsorp Mini (Bel, Japan). Prior to the analysis, approximately 30 mg of sample were evacuated at 90 °C under primary vacuum overnight. Thermogravimetry analyses (TGA) were performed on a Mettler Toledo TGA/DSC 1, STARe System apparatus under oxygen flow (50 mL min⁻¹) at a heating rate of 3 °C min⁻¹ up to 700 °C. UV-vis spectra were recorded on a Perkin Elmer Lambda 750 UV/Vis/NIR spectrometer. Scanning electronic microscopy (SEM) were performed on a JSM 7001 F microscope. HRMS was performed with a XEVO-QTOF Mass Spectrometer.

Photocatalysis experiments. 2 mg of catalyst and 2 mL of a $\text{CH}_3\text{CN}/\text{TEOA}$ (10:1) mixture were added to a 4 mL sealed quartz cuvette and sonicated for 10 min. The cuvette was then submitted to a CO_2 flux for 20 min before being irradiated for 4 h with a 280 W Xenon arc lamp (Newport) equipped with a 415 nm UV cut-off (Newport) and a temperature-controlled block at 20 °C. Gas products were analysed via gas chromatography while liquid products were assessed by ionic chromatography. In particular, H_2 measurements (aliquots of 50 µL of the headspace) were performed by gas chromatography on a Shimadzu GC-2014 equipped with a Quadrex column and a Thermal Conductivity Detector and using N_2 as a carrier gas. Formate was determined using a Metrohm 883 Basic IC plus ionic exchange chromatography instrument, using a Metrosep A Supp 5 column and a conductivity detector. After the catalytic process, the catalyst was recollected by centrifugation, dispersed in 2 mL of milli-Q water and stirred at 60 °C for 1 h. An aliquot of the liquid phase was collected and analysed by ionic chromatography to quantify the remaining formate leached by the MOF.

Steady-state photoreduction sample preparation. Prior to photoreduction experiments, approximately 0.5 mg-1mg of MOF-545(fb/Zn) or nMOF-545(Fe) was added to a 6-dram vial and suspended with a $\text{CH}_3\text{CN}/\text{TEOA}$ (10:1) solution. The vial contents were then sonicated for 1-2 min and transferred to a custom optical cell (Quark Glass, 1.0 cm pathlength), with a female 24/40 joint. A stir bar was added to the optical cell and a rubber septum was used to seal the joint. The suspension was then degassed with Ar for 20-30 min away from light. Afterwards, the rubber septum was wrapped with parafilm to prevent air leaks. The dissolved homogeneous molecular catalysts preparations followed the same protocol, with the only difference being the solvent matrix. For TCPP and (Zn)TCPP, a DMF/TEOA (10:1) matrix was used to dissolve the solids, whereas the FeTCPPCl sample was able to reasonably dissolve with $\text{CH}_3\text{CN}/\text{TEOA}$ (10:1).

Steady-state photoreduction measurements. The photoreduction measurements were performed with a 350 W Xe arc lamp (Newport, SP66921-5513) using a water IR filter (Newport, 6123NS), and a 395nm cut-on glass filter (Newport, FSQ-GG395). The samples were stirred approximately 2 ft from the arc lamp lens. At each time interval (1-10 min), the sample was removed from stirring and placed in the sample chamber of a Cary 5000 UV-Vis-NIR spectrometer (Agilent) to measure the electronic absorption spectrum. After the measurement, the sample was placed back in front of the arc lamp, where it remained until the next spectral measurement. Measurements were ceased when no spectral changes were observed over three-time intervals.

Steady-state and time-resolved emission measurements. The steady-state emission spectra were obtained using a QuantaMaster Model QM-200-4E emission spectrophotometer from Photon Technology, Inc. (PTI). The excitation light source was a 75 W Xe arc lamp (Newport). The detector was a thermoelectrically cooled Hamamatsu 1527 photomultiplier tube (PMT). Time-resolved fluorescence lifetimes were obtained *via* the time-correlated single photon counting technique (TCSPC) with the same QuantaMaster Model QM-200-4E emission spectrophotometer from Photon Technology, Inc. (PTI) equipped with a 415 nm LED and a Becker & Hickl GmbH PMH-100 PMT detector with time resolution of <220 ps FWHM. The instrument response function (1.5 ns FWHM) was measured at 415 nm using a dilute suspension of BaSO₄ in water. Kinetic deconvolutions with the instrument response function were fit using the Edinburgh Instruments L900 software suite. All other data was processed in OriginPro.

Sample preparation for transient absorption measurements. Samples were prepared by adding approximately 3 mg of MOF-545 or MOF-545(Zn) and 50 mg of NH₂-bisterminated polyethylene glycol (1500 M_n PEGNH₂) to a 2-dram vial. Then, 3 mL of anhydrous DMF were added to the vial and the contents were sonicated for 15 min. The suspension was then passed through a 450 nm PTFE syringe filter (VWR) to isolate the smaller particles. The filtrate was transferred into an optical cell and diluted with DMF until it provided an absorbance of 1.5-2.0 at the Soret band maximum. The solutions were then sealed with a rubber septum, degassed with Ar for 20-30 min and then used in the experiments. The errors associated with each measurement are the standard deviations from multiple measurements.

Transient absorption measurements. Steady-state and time-resolved transient absorption measurements were conducted with an Edinburgh Instruments LP980 laser flash photolysis system. The excitation source was a dye laser (Sirah CobraStretch) circulating a 1,4-dioxane solution of Exalite 417 (Exciton, Inc.) which exhibits tuneable lasing from 414-422 nm and was varied within this range to attain optimal sample absorption/remove scatter when probing the Soret band bleaches. The pump source for the dye laser was a frequency tripled (355 nm) Spectra-Physics Quanta-Ray INDI Nd:YAG laser, operating at 1Hz with a 6-8 ns pulse width. The spectrometer was equipped with an Andor i-Star ICCD camera for steady-state measurements and a Hamamatsu R928 PMT for measuring single wavelength kinetics. The white light source was a pulsed 150 W XBO Xe arc lamp. The average energy per pulse was kept at 0.5-1 mJ for solution measurements and 2-3 mJ for MOF suspensions. Sample stability was monitored via UV-Vis before and after measurements. For spectral absorption mappings, time-zero was defined as the emission signal after the exciting laser pulse disappeared from the emission spectrum. The reported single-wavelength kinetic lifetimes were averaged over multiple trials. The MOF kinetic traces were subjected to a 5-point (40ns/point) moving

average for clarity. The ratio of 5:5:1 was chosen so that the sum of the two solvent ratios (CH_3CN and H_2O) would be 10, to mimic that of 10:1 $\text{CH}_3\text{CN}/\text{TEOA}$.

HEPES buffer preparation. The 5:5:1 (v/v/v) $\text{CH}_3\text{CN}/(\text{HEPES}/\text{H}_2\text{O})/\text{TEOA}$ buffer was prepared by adding Na-HEPES (1.432 g, 5.5 mmol) and HEPES acid (464.8 mg, 1.95 mmol) into 25 mL deionized water to yield a pH of ~8. To this solution, 25 mL of CH_3CN and 5 mL TEOA were then added and stirred to homogeneity. The pH of the final solution was ~9.3.

XPS measurements. XPS surface chemical analyses were carried out with a Thermo Fisher Scientific Nexsa spectrometer using a monochromatic Al K α X-Ray source (1486.6 eV) and a dual flood gun (low energy electron and ion). A 400 μm X-ray spot was focused on a small amount of NanoMOF-545(Fe) compound previously placed onto a carbon tape. Survey spectra were acquired using a Constant Analyser Energy (CAE) mode of 200 eV and an energy step size of 1 eV. Core levels spectra of interest were acquired using a CAE mode of 50 eV and an energy step size of 0.1 eV. Data were then processed using Thermo Fisher Scientific Avantage \circledR software. Quantification was obtained from the photopeak areas after a Shirley type background subtraction and the use of “ALTHERMO1” library as sensitivity factor collection. All the binding energies were corrected with respect to the position of the C-C contribution at 284.8 eV from the C1s spectrum. Spectrometer energy calibration is accomplished according to Thermo Fisher Scientific procedure using metallic Cu, Ag and Au internal references.

Characterisation of the MOF-545(TM) series of catalysts. The IR spectrum of NanoMOF-545(Fe) exhibits the characteristic Fe-N vibration at 997 cm^{-1} , close to that of MOF-545(Fe) (1001 cm^{-1}) (Figure S2).⁴ Persistence of porphyrin metalation during MOF synthesis was attested by EDX measurements (see Experimental section above). Thermogravimetric analysis (TGA) curves of NanoMOF-545 and NanoMOF-545(Fe) are depicted in Figure S4, showing weight losses at 500°C of 67.9% and 65.8%, respectively. These weight losses are assigned to linker decomposition along with the formation of inorganic oxides, the experimental values agreeing with those predicted from the molecular formula (69.0% and 64.5%, respectively). The N₂ adsorption/desorption isotherms of MOF-545(Fe), NanoMOF-545 and NanoMOF-545(Fe) have been measured (Figure S5). A Brunauer–Emmett–Teller (BET) surface area of 1434 $\text{m}^2 \text{g}^{-1}$ was determined for NanoMOF-545(Fe), on par with those determined for MOF-545(Fe) (1396 $\text{m}^2 \text{g}^{-1}$) and NanoMOF-545 (1698 $\text{m}^2 \text{g}^{-1}$). Finally, the pore diameters of all these materials are similar, with two types of pores of ca. 1.7 and 3.7 nm sizes.

In order to confirm the oxidation state of the Fe ions in the porphyrin linkers, XPS analyses were conducted on nanoMOF-545(Fe). The Fe2p spectral region presented in Figure S6a shows two peaks centred at 710.2 and 723.3 eV attributed to Fe2p_{3/2} and Fe2p_{1/2}, respectively. The comparison of this spectrum with that of Fe₂O₃ recorded in similar conditions clearly indicates that the iron atoms are in the +III oxidation state in the nanoMOF-545(Fe) compound. We also explored the Zr3d core level. Two contributions were observed at 183.1 and 185.4 eV associated to Zr3d_{5/2} and Zr3d_{3/2} respectively (Figure S6b). These positions in binding energies are fully consistent with the ones expected for Zr(IV) ions.

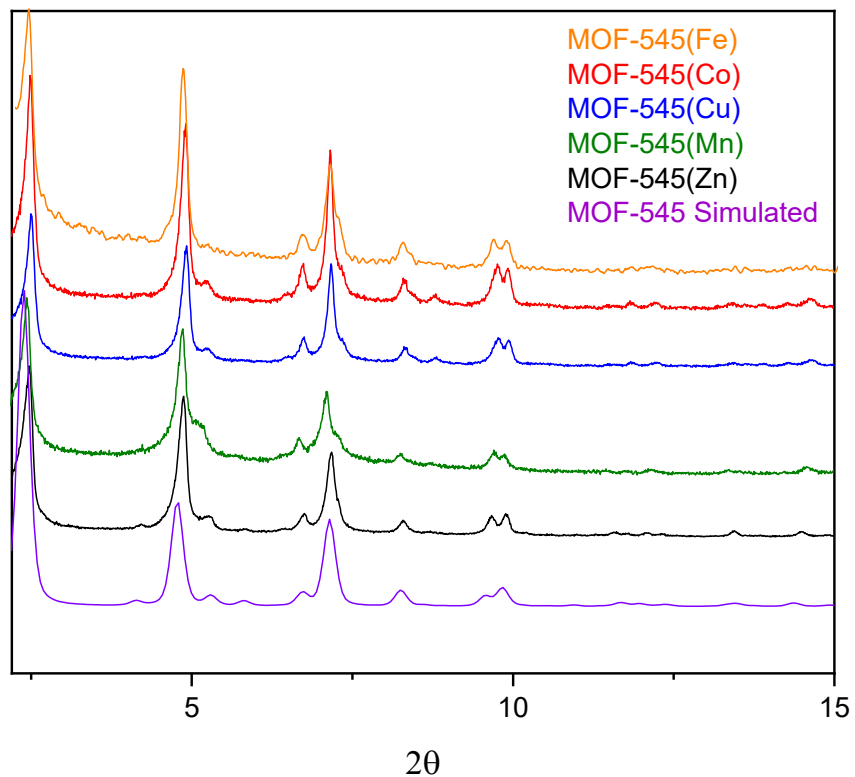


Figure S1. (a) Comparison of the experimental X-ray powder patterns of MOF-545(Fe) (orange), MOF-545(Co) (red), MOF-545(Cu) (blue), MOF-545(Mn) (green), MOF-545(Zn) (black) and of the simulated powder pattern of MOF-545 (purple).

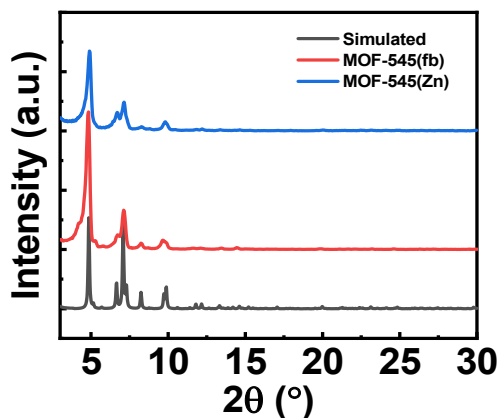


Figure S1 (b). PXRD pattern of MOF-545 (red), and MOF-545(Zn) (blue) used in photophysical measurements. Simulated MOF-545 powder pattern (black).

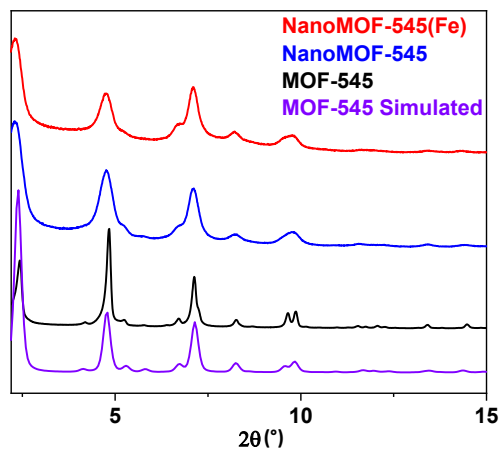


Figure S1 (c). Comparison of the experimental PXRD patterns of NanoMOF-545(Fe) (red), and NanoMOF-545 (blue), MOF-545 (black)and the simulated MOF-545 powder pattern (purple).

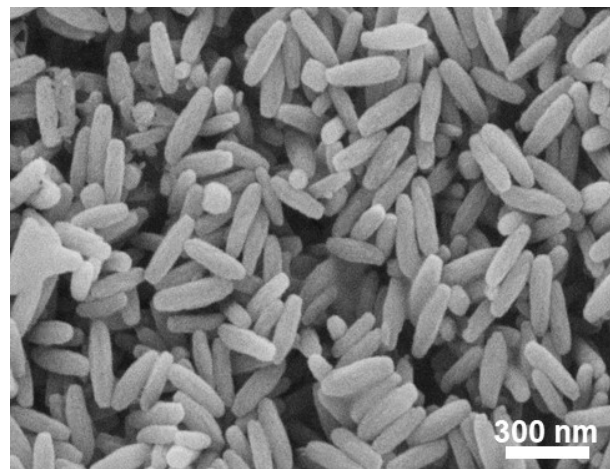


Figure S1 (d). SEM image of MOF-545 used for photophysical measurements. Image obtained by Xiaozhou Yang at Virginia Tech.

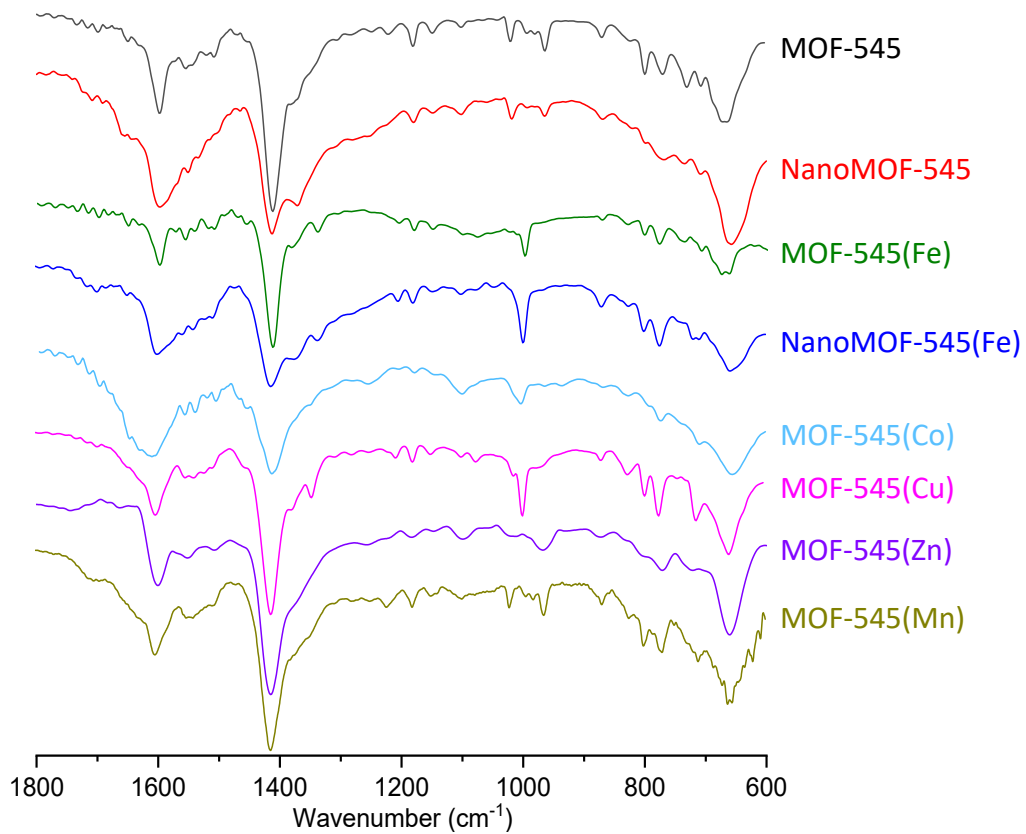


Figure S2. FT-IR spectra of MOF-545 (black), NanoMOF-545 (red), MOF-545(Fe) (green), NanoMOF-545(Fe) (blue), MOF-545(Co) (cyan), MOF-545(Cu) (pink), MOF-545(Zn) (purple) and MOF-545(Mn) (khaki).

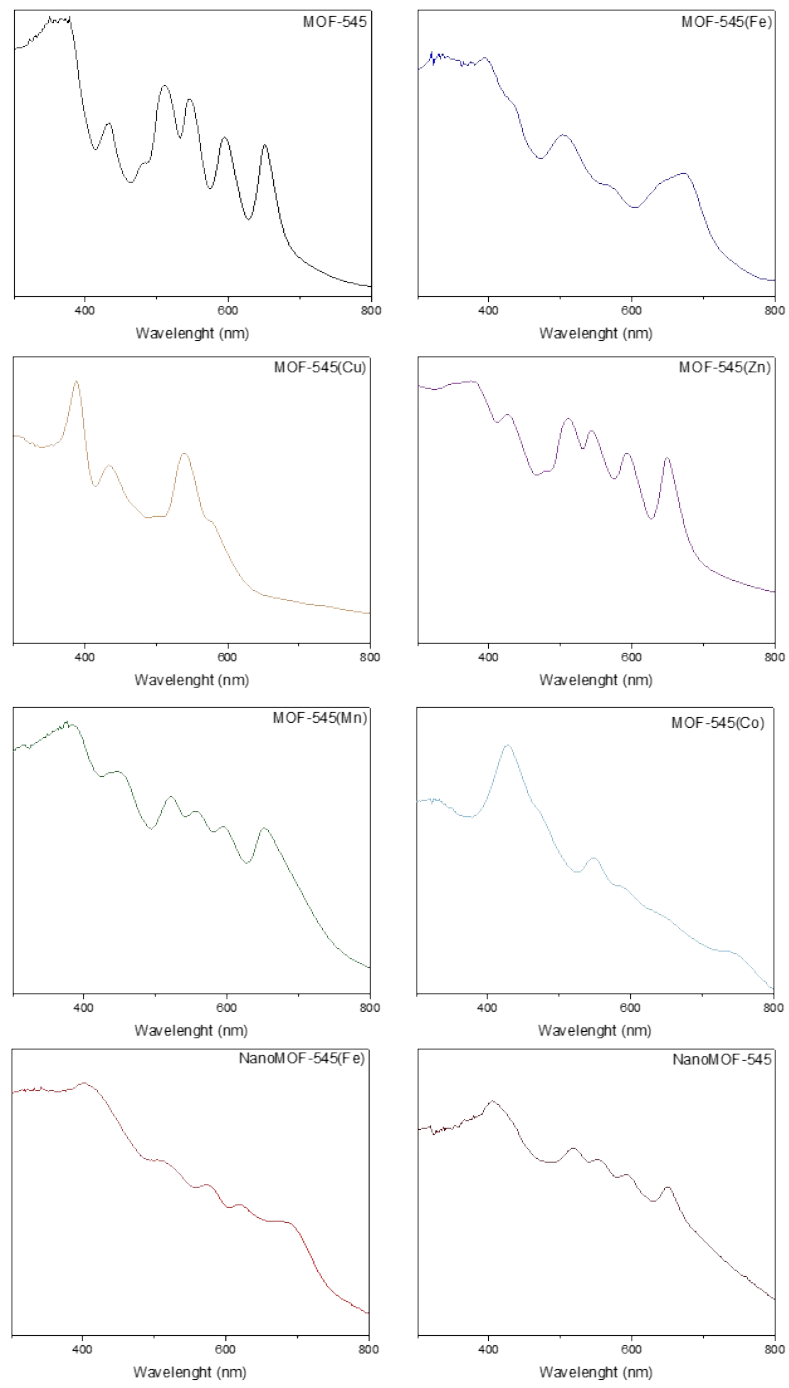


Figure S3. UV-visible absorption spectra of MOF-545 (black), MOF-545(Fe) (blue), MOF-545(Cu) (orange), MOF-545(Zn) (purple), MOF-545(Mn) (green), MOF-545(Co) (cyan), NanoMOF-545 (brown) and NanoMOF-545(Fe) (red).

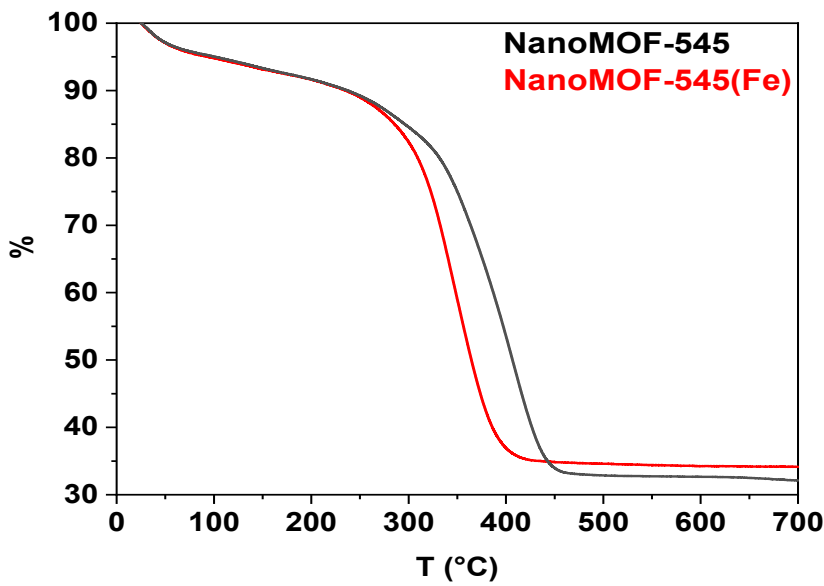


Figure S4. TGA curves of NanoMOF-545 (black) and NanoMOF-545(Fe) (red).

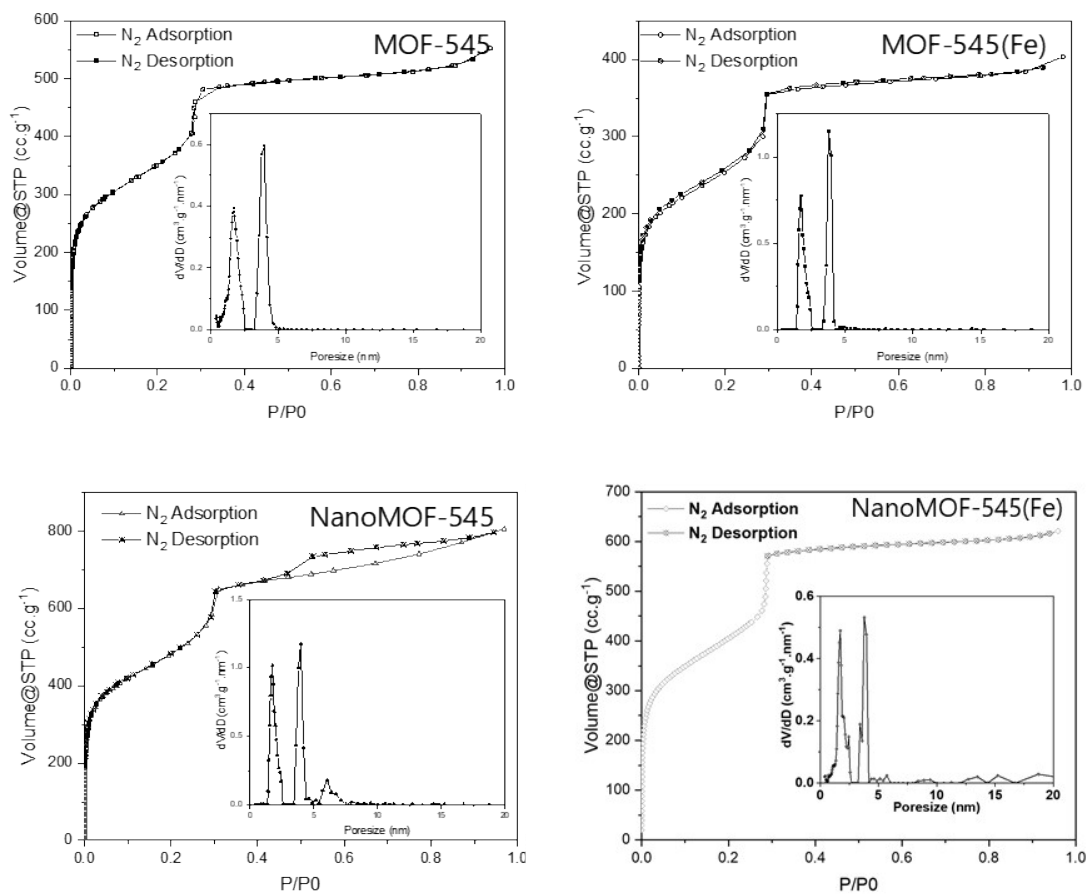


Figure S5. BET N_2 adsorption/desorption isotherms (77 K, $P/P_0 = 1 \text{ atm.}$) of MOF-545, MOF-545(Fe), NanoMOF-545 and NanoMOF-545(Fe). Insert: pore size distributions.

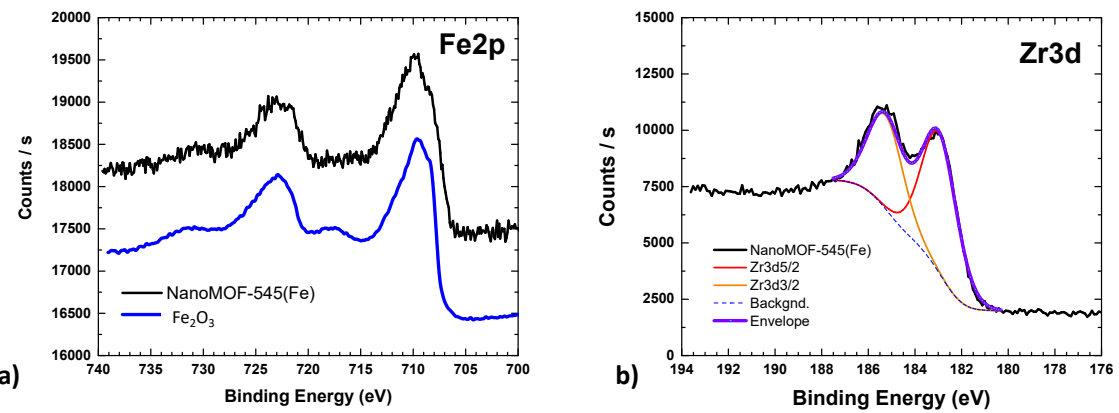


Figure S6. XPS spectra recorded on NanoMOF-545(Fe): a) Fe2p spectral region of NanoMOF545(Fe) and of Fe_2O_3 as a comparison; b) Zr3d spectral region.

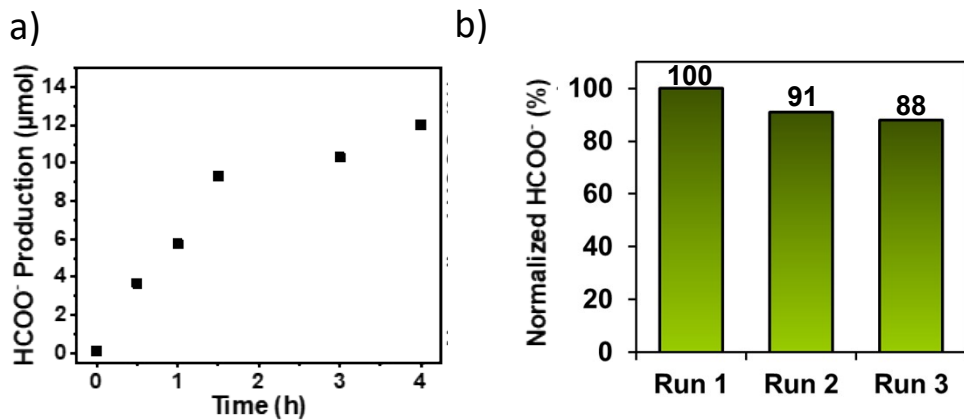


Figure S7. a) Time evolution of the visible-light-driven formate production for NanoMOF-545(Fe); b) Recyclability experiments for NanoMOF(Fe). Reaction conditions: catalyst 2 mg, $\text{CH}_3\text{CN}/\text{TEOA}$ (10:1) 2 mL ($\lambda > 415$ nm, 280 W). Photocatalytic tests were performed up to 20 h showing that a *plateau* in the photocatalytic activity is reached at 4 h. We further understood the origin of the *plateau* as the result of the formate product remaining adsorbed in the MOF (see main text). This observation is indeed consistent not only with the proposed mechanism whereby formate may remain coordinated to the Zr-oxoclusters - its release being endergonic- but also with the fact that the MOF photocatalyst, once regenerated through successive washing steps, can be reused as shown in b).

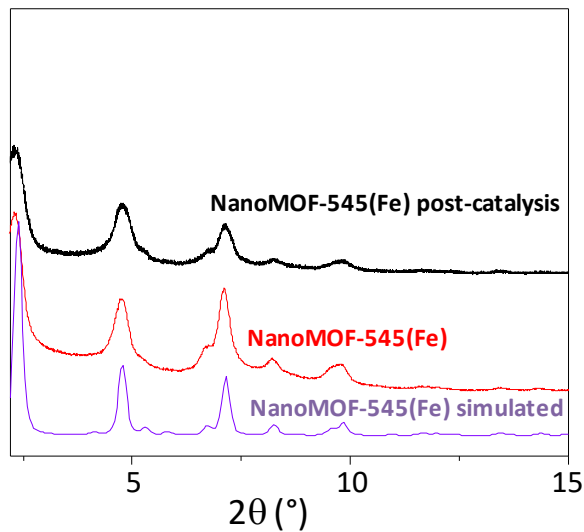


Figure S8: PXRD pattern of MOF-545 simulated (purple), NanoMOF-545(Fe) before catalysis (red) and after 4 h catalytic run (black).

Table S1: Photocatalytic reduction of CO₂ with 2 mg of MOF-545(TM) catalyst in 2 mL of CH₃CN/TEOA (10:1, v/v) under 280 W Xe lamp irradiation for 4h ($\lambda > 415$ nm). The formate was measured without desorbing protocol.

Catalyst	Comment	Formate (μmol)	Rate $\mu\text{mol g}^{-1} \text{h}^{-1}$
-	No catalyst	0.26	-
MOF-545	No light	0.34	42
MOF-545	No TEOA	0.35	44
MOF-545	No CO ₂	0.34	42
MOF-545		1.28	159
MOF-545(Cu)		1.34	167
MOF-545(Co)		1.80	225
MOF-545(Mn)		3.34	382
MOF-545(Zn)		3.50	417
MOF-545(Fe)		4.52	566
NanoMOF-545		3.20	400
NanoMOF-545(Fe)		9.28	1160

Table S2. Comparison of HCOO^- production from photocatalytic CO_2 reduction by MOF-based photocatalytic systems.

Material	Wavelength (nm)	External Photosensitizer	Reaction medium	HCOOH production ($\mu\text{mol g}^{-1} \text{h}^{-1}$)	Ref.
Zr-MOFs					
NanoMOF-545(Fe)	>415	-	$\text{CH}_3\text{CN}/\text{TEOA}$ (10:1)	1500	This work
MOF-545(Fe)	>415	-	$\text{CH}_3\text{CN}/\text{TEOA}$ (10:1)	566	This work
MOF-545(Zn)	>415	-	$\text{CH}_3\text{CN}/\text{TEOA}$ (10:1)	417	This work
NanoMOF-545	>415	-	$\text{CH}_3\text{CN}/\text{TEOA}$ (10:1)	400	This work
MOF-545(Mn)	>415	-	$\text{CH}_3\text{CN}/\text{TEOA}$ (10:1)	382	This work
MOF-545(Co)	>415	-	$\text{CH}_3\text{CN}/\text{TEOA}$ (10:1)	225	This work
MOF-545(Cu)	>415	-	$\text{CH}_3\text{CN}/\text{TEOA}$ (10:1)	167	This work
MOF-545	>415	-	$\text{CH}_3\text{CN}/\text{TEOA}$ (10:1)	159	This work
PCN-222(Ni) (MOF-545(Ni))	420-800	-	$\text{CH}_3\text{CN}/\text{TEOA}$ (10:1)	373	Dehghanpour and coll. <i>Appl. Organomet. Chem.</i> 2021 , e6422
PCN-222(Fe) (MOF-545(Fe))	420-800	-	$\text{CH}_3\text{CN}/\text{TEOA}$ (10:1)	347	Dehghanpour and coll. <i>Appl. Organomet. Chem.</i> 2021 , e6422
PCN-222(Cu) (MOF-545(Cu))	420-800	-	$\text{CH}_3\text{CN}/\text{TEOA}$ (10:1)	333	Dehghanpour and coll. <i>Appl. Organomet. Chem.</i> 2021 , e6422
PCN-222(Co) (MOF-545(Co))	420-800	-	$\text{CH}_3\text{CN}/\text{TEOA}$ (10:1)	313	Dehghanpour and coll. <i>Appl. Organomet. Chem.</i> 2021 , e6422
PCN-222 (MOF-545)	420-800	-	$\text{CH}_3\text{CN}/\text{TEOA}$ (10:1)	173	Dehghanpour and coll. <i>Appl. Organomet. Chem.</i> 2021 , e6422
PCN-222 (MOF-545)	420-800	-	$\text{CH}_3\text{CN}/\text{TEOA}$ (10:1)	120	Zhang, Liang and coll. <i>J. Am. Chem. Soc.</i> 2015 , 137, 13440
PCN-224	420-800	-	Ethyleneglycol 20 mM	45.2	Jin <i>New. J. Chem.</i> 2020 , 44, 15362
PCN-222 (MOF-545)	420-800	-	Ethyleneglycol 20 mM	10.2	Jin <i>New. J. Chem.</i> 2020 , 44, 15362
PCN-222(Zn) (MOF-545(Zn))	420-800	-	Ethyleneglycol 20 mM	120.2	Jin <i>New. J. Chem.</i> 2020 , 44, 15362
PCN-224	>400	-	$\text{CH}_3\text{CN}/\text{TEOA}$ (4:1)	25	Zhang and coll. <i>Applied. Catal. B: Environmental</i> 2018 , 231, 173
PCN-136	>420	-	$\text{CH}_3\text{CN}/\text{H}_2\text{O}/\text{TIPA}^a$ (40:5:5)	45	Lan, Alsalme, Zhou and coll. <i>J. Am. Chem. Soc.</i> 2019 , 141, 2054
Rh-PMOF-1	>400	-	$\text{CH}_3\text{CN}/\text{TEOA}$ (4:1)	74	Zhang and coll. <i>Applied. Catal. B: Environmental</i> 2018 , 231, 173
NH₂-UiO-66	420-800	-	$\text{CH}_3\text{CN}/\text{TEOA}$ (5:1)	26.4	Li and coll., <i>Chem. Eur. J.</i> 2013 , 19, 14279
NNU-28	420-800	-	$\text{CH}_3\text{CN}/\text{TEOA}$ (30:1)	52.8	Xing, Zu and coll., <i>J. Mat. Chem. A</i> 2016 , 4, 2657
Zr-MOFs functionalized via Post Synthetic Exchange					
Cp*Rh@UiO-67	415-800	[Ru(bpy) ₃]Cl ₂	$\text{CH}_3\text{CN}/\text{TEOA}$ (5:1)	464 ^b	Fontecave and coll. <i>ChemSusChem.</i> 2015 , 8, 603
UiO-66-CrCAT	420-800	-	$\text{CH}_3\text{CN}/\text{TEOA}$ (4:1), BNAH	1724	Kang, Cohen and coll. <i>Chem. Commun.</i> 2015 , 51, 16549
NH₂-UiO-66(Zr/Ti)	420-800	-	$\text{CH}_3\text{CN}/\text{TEOA}$ (4:1), BNAH	1052	Kang, Cohen and coll. <i>Chem. Commun.</i> 2015 , 51, 5735
Other MOFs					
NH₂-MIL-125(Ti)	420-800	-	$\text{CH}_3\text{CN}/\text{TEOA}$ (5:1)	16.28	Li and coll. <i>Angew. Chem. Int. Ed.</i> 2012 , 51, 3364
MIL-101(Fe)	420-800	-	$\text{CH}_3\text{CN}/\text{TEOA}$ (5:1)	147.5	Li and coll. <i>ACS Catal.</i> 2014 , 4, 4254

a: TIPA = triisopropanolamine

b: H₂ is also produced (selectivity in formate is 57%)

2. Analysis of the evolution of UV spectra with time / photophysical measurements.

Shown in Figure S9a are the steady-state emission spectra of MOF-545 and MOF-545(Zn). For completion, those of free-base and metalated porphyrin ligands in solution are shown below (Figure S11). The emission spectrum of MOF-545 shows the typical two emission bands associated with TCPP excited states at 647 nm ($S_{10}^* \rightarrow S_{00}$) and 712 nm ($S_{10}^* \rightarrow S_{01}$), while for MOF-545(Zn), the bands occur at 607 nm and 656 nm (see Figures S10-11). Note that MOF-545(Zn) showed a higher emission intensity at the 656 nm band as compared to that of (Zn)TCPP in solution, likely due to the presence of a minor amount of unmetalated TCPP impurity.

To establish the excited singlet state lifetime for both MOFs, we analysed the time-correlated single photon counting (TCSPC) decay curves for MOF-545 and MOF-545(Zn), (Figure S9b), which revealed the coexistence of two types of porphyrin linkers in the MOFs.^{5,6} On the one hand, MOF-545 exhibited emission lifetimes of 1.27 ± 0.06 ns and 2.9 ± 0.2 ns (Table S3), which can be ascribed to N-protonated TCPP and native deprotonated TCPP, respectively. On the other hand, MOF-545(Zn) showed lifetimes of 474 ± 3 ps and 2.82 ± 0.06 ns (Table S3). The longer lifetime can be assigned to the aforementioned freebase impurity and the dominant short lifetime component to MOF-incorporated (Zn)TCPP. The measured singlet excited state lifetime in MOF-545(Zn) is shorter than that in MOF-545 due to spin-orbit coupling of the ring electrons with the Zn metal, thereby increasing triplet state yield over singlet formation. Note that the spectral features of both MOFs aligned quite well with their parent ligands in solution (Figures S10, S11). Spectral features of free-base and metalated porphyrin ligands are given in Figures S12-S25). It is also worth mentioning that the lifetimes in both MOFs are significantly quenched in comparison to those of the ligands in solution (Table S3) due to the rapid porphyrin-to-porphyrin energy transfer and the presence of linker-centred trap states resulting in decreased lifetimes.⁵

The solution-state emission and absorption photophysical lifetimes and parameters are summarized in Table S4. All measurements were performed in Ar-purged DMF or with a suspension-stabilizer (polyethylene glycol diamine, PEGNH₂) for control experiments. To ensure the emitting states of MOF-545 and MOF-545(Zn) arise from the linkers, excitation spectra were obtained while monitoring the emission intensity at the highest energy Q-band emission wavelength (646 nm). The excitation spectra of the MOFs (Figure S10) align quite well with the ground-state absorption spectra of the linker, indicating that the porphyrin linkers are responsible for emission in the MOF. The singlet emission spectra of TCPP and (Zn)TCPP had two emission bands between 600 and 800 nm (Figure S11).⁷ TCPP had two emission lifetimes when excited at the Soret band: 4.4 ± 0.5 ns ($15 \pm 2\%$) and 12.5 ± 0.2 ns ($85 \pm 2\%$) (Figure S12). This short lifetime component is attributed to a small population of N-protonated porphyrin species, which can act as trap states in MOF-545.⁵ This protonated population was also observed in the TCPP ground-state bleach of its TA spectrum, given the high absorptivity in the Soret region. (Zn)TCPP provided an emission lifetime of 2.17 ± 0.03 ns, aligning well with literature (Figure S13).⁷

The TA spectra of TCPP and (Zn)TCPP (Figures S14 and S15) were similar to one another; both exhibiting strong ground-state bleaches (GSB) around 420-430 nm, and excited-state absorptions (ESA) ca. 445-460 nm. The triplet kinetics at their respective GSBs and ESAs were also close to one another (Table S4), with the long TCPP lifetime component being 330 ± 30 μ s (Figure S16) and (Zn)TCPP having a lifetime of 360 ± 10 μ s (Figure S22). When the TA measurements were conducted in the presence of PEGNH₂ to see if the ligand behaviour differs, TCPP exhibited negligible spectral

changes, though the lifetimes in the excited state and bleach increased to 390 ± 30 μs (Figure S18) and 480 ± 80 μs (Figure S19), respectively. (Zn)TCPP, exhibited a more rounded triplet ESA, and a noticeably quenched triplet lifetime (Figures S23-25). The quenching of the triplet excited state of (Zn)TCPP ($350 \mu\text{s}$ to $210 \mu\text{s}$) was accompanied by the presence of a new lifetime component in the GSB ($140 \pm 10 \mu\text{s}$, $50 \pm 20 \%$, Figure S25). The new lifetime is attributed to bound PEGNH₂-Zn metal sites, because Zn too, can be axially ligated with a variety of solvents and coordinating species.⁸

Table S3. Photophysical data of MOF-545 and MOF-545(Zn) suspensions.

Sample	Fluorescence emission lifetimes				³ T excited state absorption lifetimes				³ T ground state bleach lifetimes			
			A ₁	A ₂			A ₁	A ₂			A ₁	A ₂
	τ_1	τ_2	(%)	(%)	τ_1	τ_2	(%)	(%)	τ_1	τ_2	(%)	(%)
MOF- 545	1.27 ± 0.06 ns	2.9 ± 0.2 ns	$64 \pm 7\%$	$36 \pm 7\%$	16 ± 3 μs	160 ± 30 μs	$29 \pm 4\%$	$71 \pm 4\%$	11 ± 2 μs	170 ± 20 μs	$46 \pm 8\%$	$54 \pm 8\%$
MOF- 545(Zn)	474 ± 3 ps	2.82 ± 0.06 ns	$98.50 \pm 0.08\%$	$1.50 \pm 0.08\%$	5 ± 2 μs	90 ± 20 μs	$61 \pm 2\%$	$39 \pm 2\%$	10 ± 4 μs	100 ± 20 μs	$74 \pm 3\%$	$26 \pm 3\%$
)												

Table S4. Photophysical data of TCPP and (Zn)TCPP in Ar-purged DMF solutions.

Sample	Fluorescence emission lifetimes				³ T excited state absorption lifetimes				³ T ground state bleach lifetimes			
			A ₁	A ₂			A ₁	A ₂			A ₁	A ₂
	τ_1	τ_2	(%)	(%)	τ_1	τ_2	(%)	(%)	τ_1	τ_2	(%)	(%)
TCPP	4.4 ± 0.5 ns	12.4 ± 0.1 ns	15 ± 2	85 ± 2	330 ± 30 μs	---	100	---	120 ± 20 μs	330 ± 50 μs	35 ± 10	65 ± 10
					390 ± 30 μs^*	---	100	---	180 ± 40 μs^*	480 ± 80 μs^*	50 ± 10	50 ± 10
(Zn)TCPP	2.17 ± 0.03 ns	---	100	---	350 ± 30 μs	---	100	---	360 ± 10 μs	---	100	---
					210 ± 20 μs^*	---	100	---	140 ± 10 μs^*	280 ± 40 μs^*	50 ± 20	50 ± 20

* Lifetime values of the ligand solutions in the presence of 15 mg/mL PEGNH₂.

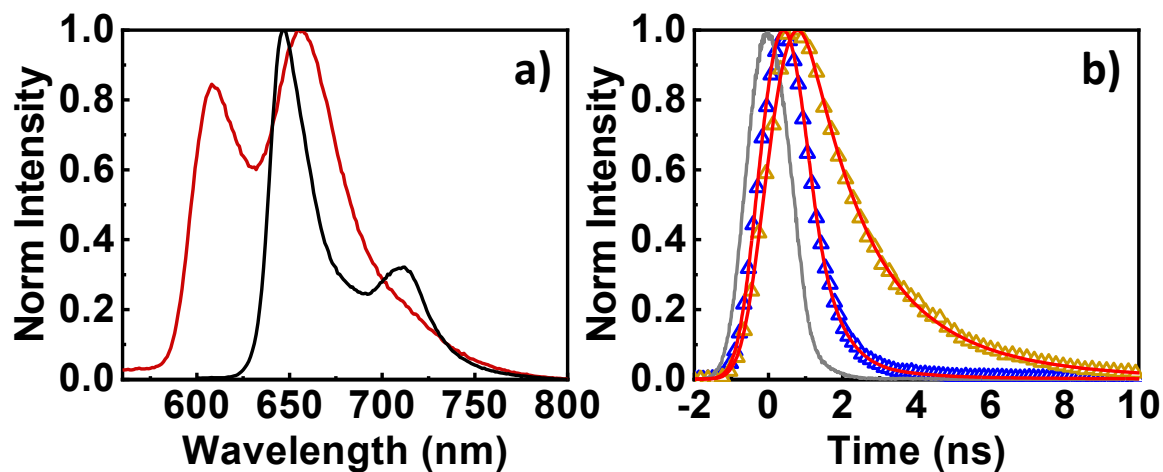


Figure S9. a) Steady-state emission spectra of MOF-545 (black) and MOF-545(Zn) (red) in degassed DMF, and b) TCSPC decay curves of MOF-545 (yellow triangles), and MOF-545(Zn) (blue triangles) in degassed DMF. The instrument response function is the gray curve. $\lambda_{\text{exc}} = 415 \text{ nm}$.

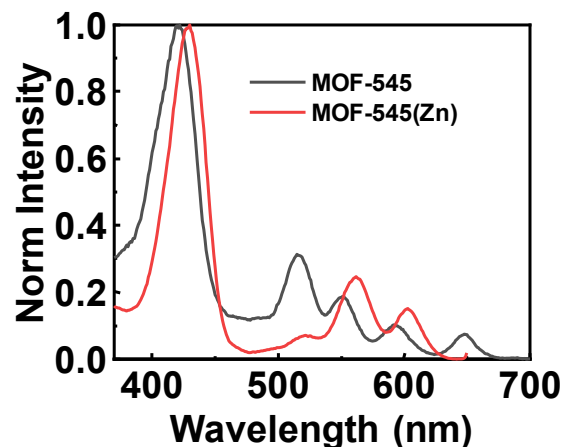


Figure S10. Steady-state excitation spectra of MOF-545 (black, $\lambda_{\text{em}} = 712 \text{ nm}$), and MOF-545(Zn) (red, $\lambda_{\text{em}} = 656 \text{ nm}$) in DMF.

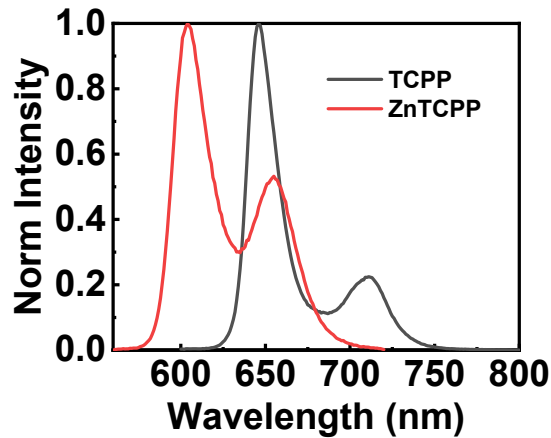


Figure S11. Steady-state emission spectra of TCPP (black), and (Zn)TCPP (red) in DMF. $\lambda_{\text{exc}} = 415$ nm from a 75 W Xe arc lamp.

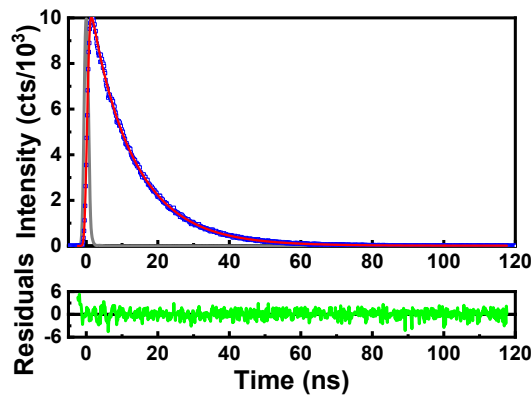


Figure S12. Emission decay trace of TCPP in DMF (blue), reconvolution fit (red) measured at 646 nm. IRF (gray) measured at $\lambda_{\text{exc}} = 415$ nm. $\tau_1 = 4.4 \pm 0.5$ ns (15 ± 2 %), $\tau_2 = 12.5 \pm 0.2$ ns (85 ± 2 %).

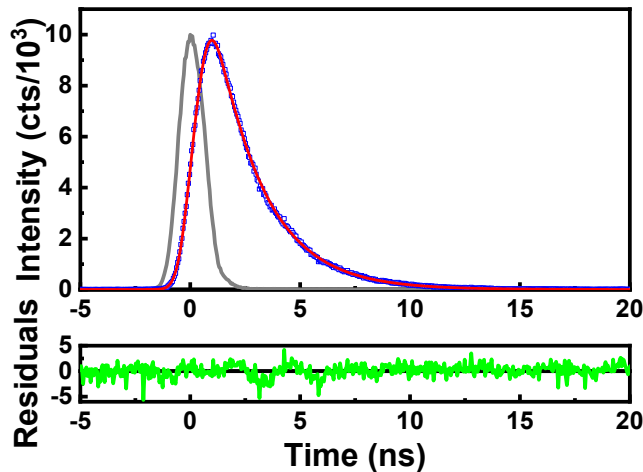


Figure S13. Emission decay trace of (Zn)TCPP in DMF (blue), reconvolution fit (red) measured at 646 nm. IRF (grey) measured at $\lambda_{\text{exc}} = 415$ nm. $\tau = 2.17 \pm 0.03$ ns

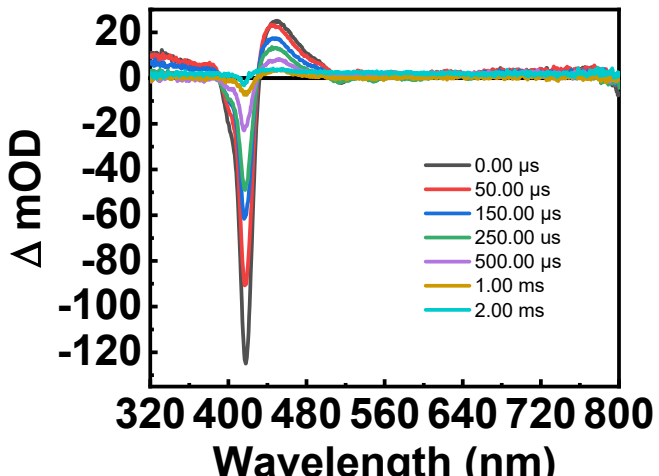


Figure S14. Transient absorption time-map of freebase TCPP in DMF. $\lambda_{\text{exc}} = 415 \text{ nm}$, 1 mJ per pulse.

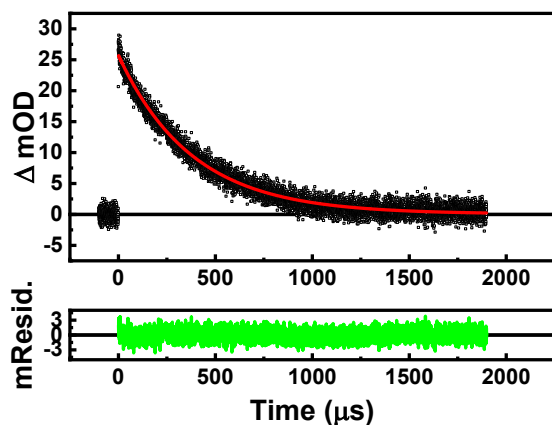


Figure S15. Excited-state absorption decay trace of freebase TCPP in DMF (black), exponential fit (red), and regular residual (green, $\times 10^3$) measured at 450 nm. $\lambda_{\text{exc}} = 415 \text{ nm}$, 1 mJ per pulse, $\tau = 330 \pm 30 \mu\text{s}$.

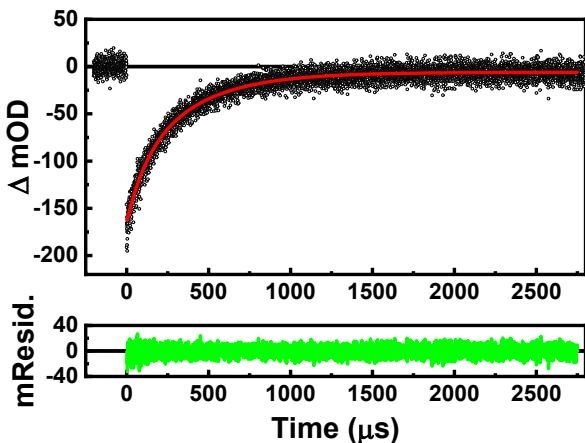


Figure S16. Ground-state bleach recovery trace of freebase TCPP in DMF (black), exponential fit (red), and regular residual (green, $\times 10^3$) measured at 419 nm. $\lambda_{\text{exc}} = 415 \text{ nm}$, 1 mJ per pulse; $\tau_1 = 120 \pm 20 \mu\text{s}$ ($35 \pm 10 \%$), $\tau_2 = 330 \pm 50 \mu\text{s}$. When probing the ground state bleach in TCPP, we often observe a short lifetime component, which we attribute to N-protonated TCPP. Both N-protonated and freebase TCPP exhibit high absorptivity at the Soret band, making it possible to see this kinetic component.

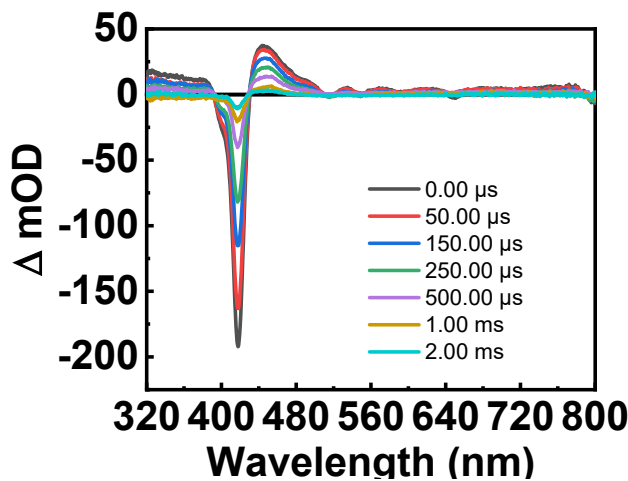


Figure S17. Transient absorption time-map of freebase TCPP in a 15 mg/mL solution of PEGNH₂ (1500 M_n) in DMF. $\lambda_{\text{exc}} = 415 \text{ nm}$, 1 mJ per pulse.

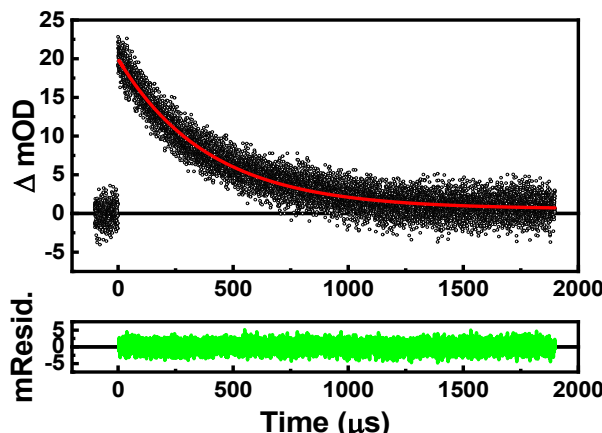


Figure S18. Excited-state absorption decay trace of freebase TCPP in a 15 mg/mL solution of PEGNH₂ (1500 M_n) in DMF (black), exponential fit (red), and regular residual (green, $\times 10^3$) measured at 460 nm. $\lambda_{\text{exc}} = 415 \text{ nm}$, 1 mJ per pulse; $\tau = 390 \pm 30 \mu\text{s}$.

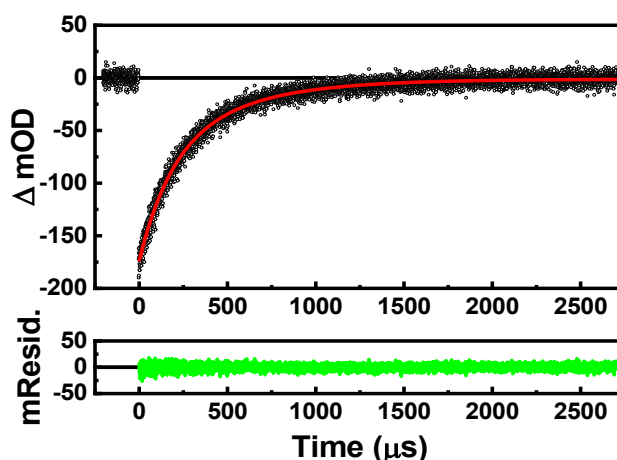


Figure S19. Ground-state bleach recovery trace of freebase TCPP in a 15 mg/mL solution of PEGNH₂ (1500 M_n) in DMF (black), exponential fit (red), and regular residual (green, $\times 10^3$) measured at 419 nm. $\lambda_{\text{exc}} = 415 \text{ nm}$, 1 mJ per pulse; $\tau_1 = 180 \pm 40 \mu\text{s}$ ($50 \pm 10 \%$), $\tau_2 = 480 \pm 80 \mu\text{s}$.

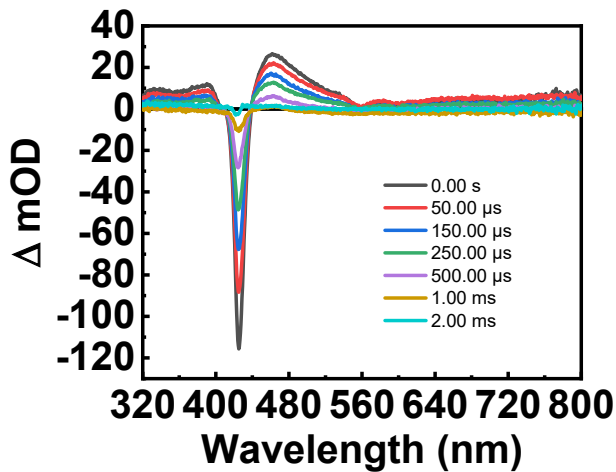


Figure S20. Transient absorption time-map of (Zn)TCPP in DMF. $\lambda_{\text{exc}} = 422 \text{ nm}$, 1 mJ per pulse.

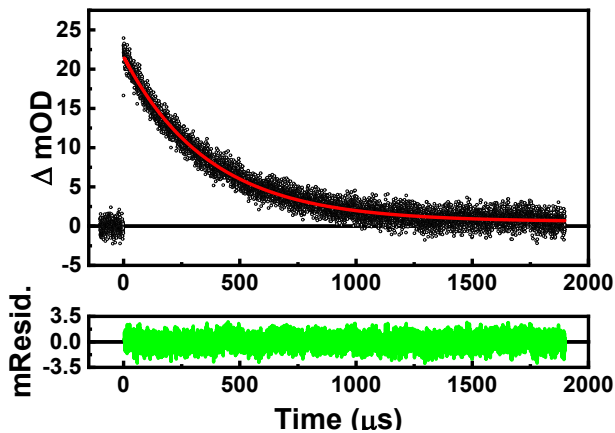


Figure S21. Excited-state absorption decay trace of (Zn)TCPP in DMF (black), exponential fit (red), and regular residual (green, $\times 10^3$) measured at 460 nm. $\lambda_{\text{exc}} = 422 \text{ nm}$, 1 mJ per pulse, $\tau = 350 \pm 30 \mu\text{s}$.

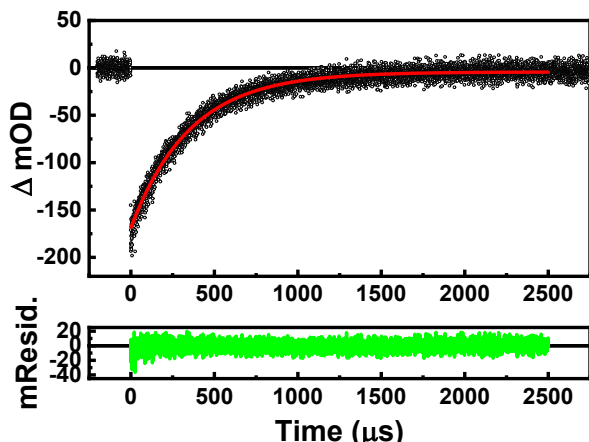


Figure S22. Ground-state bleach recovery trace of (Zn)TCPP in DMF (black), exponential fit (red), and regular residual (green, $\times 10^3$) measured at 427 nm. $\lambda_{\text{exc}} = 422 \text{ nm}$, 1 mJ per pulse; $\tau = 360 \pm 10 \mu\text{s}$.

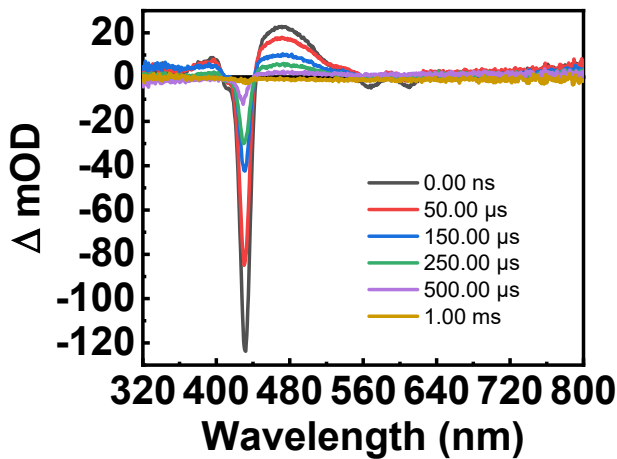


Figure S23. Transient absorption time-map of (Zn)TCPP in a 15 mg/mL solution of PEGNH₂ (1500 M_n) in DMF. $\lambda_{\text{exc}} = 422$ nm, 1 mJ per pulse.

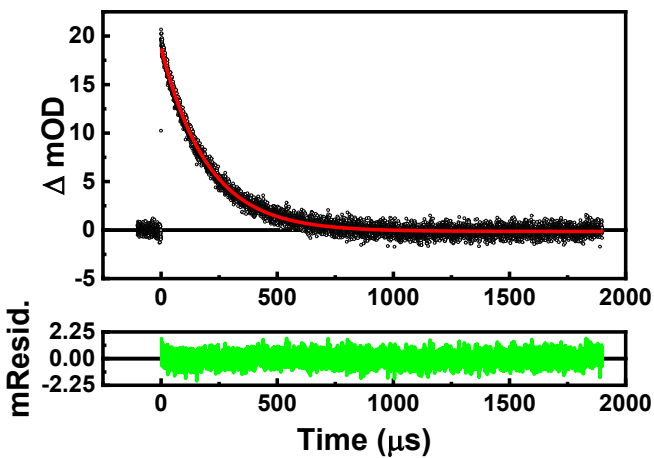


Figure S24. Excited-state absorption decay trace of (Zn)TCPP in a 15 mg/mL solution of PEGNH₂ (1500 M_n) in DMF (black), exponential fit (red), and regular residual (green, $\times 10^3$) measured at 460 nm. $\lambda_{\text{exc}} = 422$ nm, 1 mJ per pulse, $\tau = 210 \pm 20$ μ s.

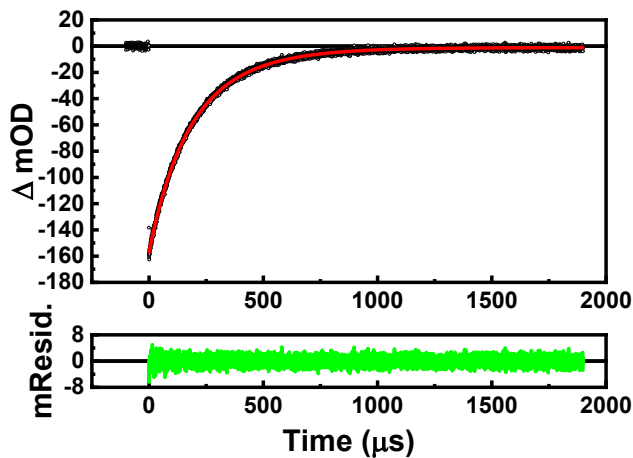


Figure S25. Ground-state bleach recovery trace of (Zn)TCPP in a 15 mg/mL solution of PEGNH₂ (1500 M_n) in DMF (black), exponential fit (red), and regular residual (green, $\times 10^3$) measured at 430 nm. $\lambda_{\text{exc}} = 422$ nm, 1 mJ per pulse; $\tau_1 = 140 \pm 10$ μ s (50 ± 20 %), $\tau_2 = 280 \pm 40$ μ s.

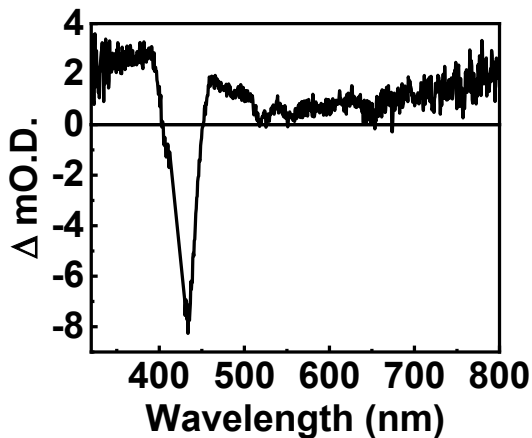


Figure S26. Steady-state transient absorption spectrum of MOF-545 in a solution of 15 mg/mL bis-terminated PEGNH₂ in DMF. $\lambda_{\text{exc}} = 422$ nm, 3 mJ per pulse. There was a slight presence of laser light in the spectrum, so those associated data points were omitted.

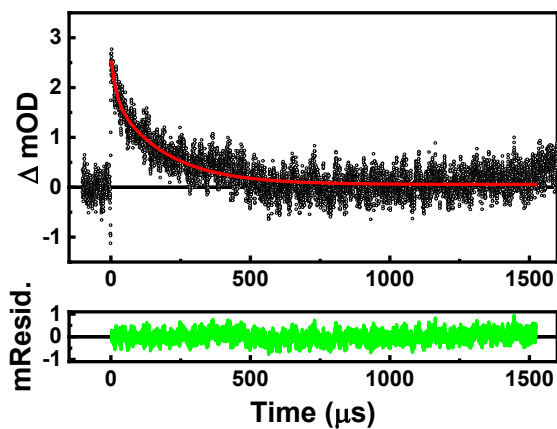


Figure S27. Excited-state absorption decay trace of MOF-545 in a solution of 15 mg/mL bis-terminated PEGNH₂ in DMF (black), exponential fit (red), and regular residual (green, $\times 10^3$) measured at 450 nm. $\lambda_{\text{exc}} = 422$ nm, 1 mJ per pulse; $\tau_1 = 16 \pm 3 \mu\text{s}$ ($29 \pm 4 \%$), $\tau_2 = 160 \pm 30 \mu\text{s}$ ($71 \pm 4 \%$).

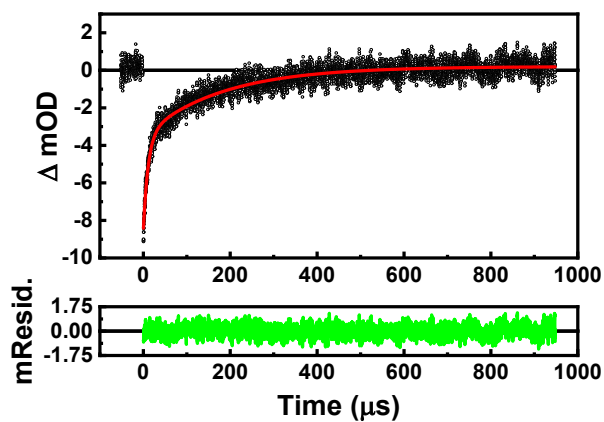


Figure S28. Ground-state bleach recovery trace of MOF-545 in a solution of 15 mg/mL bis-terminated PEGNH₂ in DMF (black), exponential fit (red), and regular residual (green, $\times 10^3$) measured at 419 nm. $\lambda_{\text{exc}} = 422$ nm, 3 mJ per pulse; $\tau_1 = 11 \pm 2 \mu\text{s}$ ($46 \pm 8 \%$), $\tau_2 = 170 \pm 20 \mu\text{s}$ ($54 \pm 8 \%$).

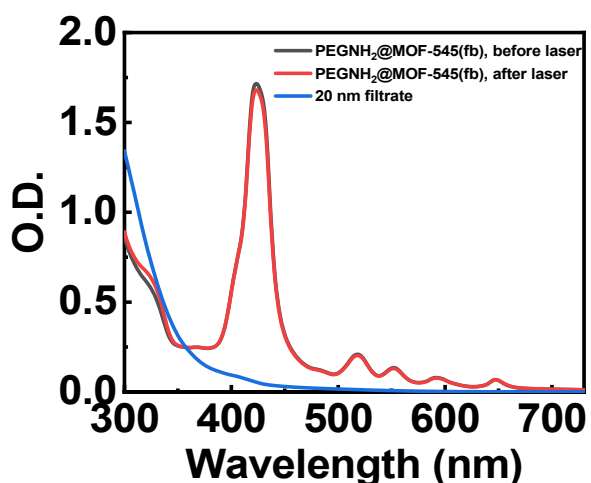


Figure S29. Steady-state electronic absorption spectra of MOF-545 in a solution of 15 mg/mL bis-terminated PEGNH_2 in DMF prior to transient absorption measurements (black), after transient absorption measurements (red), and the 20-nm syringe-filtered MOF suspension after laser measurements (blue). The upward absorption of the blue trace is due to the PEGNH_2 that passed through the filter, while the MOF was caught by the filter, as evidenced by the lack of porphyrin spectral features in the trace.

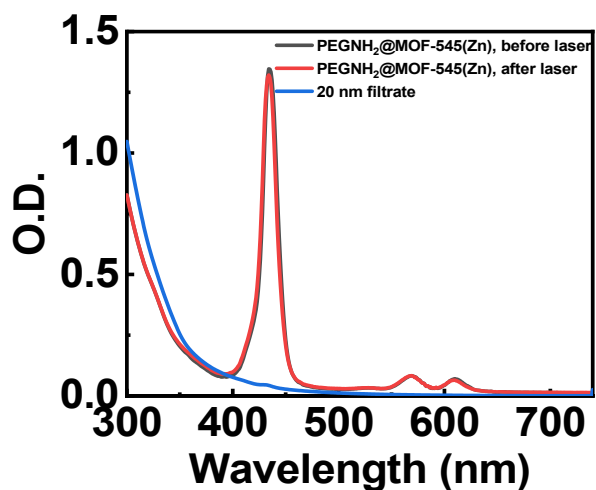


Figure S30. Steady-state electronic absorption spectra of MOF-545(Zn) in a solution of 15 mg/mL bis-terminated PEGNH_2 in DMF prior to transient absorption measurements (black), after transient absorption measurements (red), and the 20-nm syringe-filtered MOF suspension after laser measurements (blue).

3. Computational results.

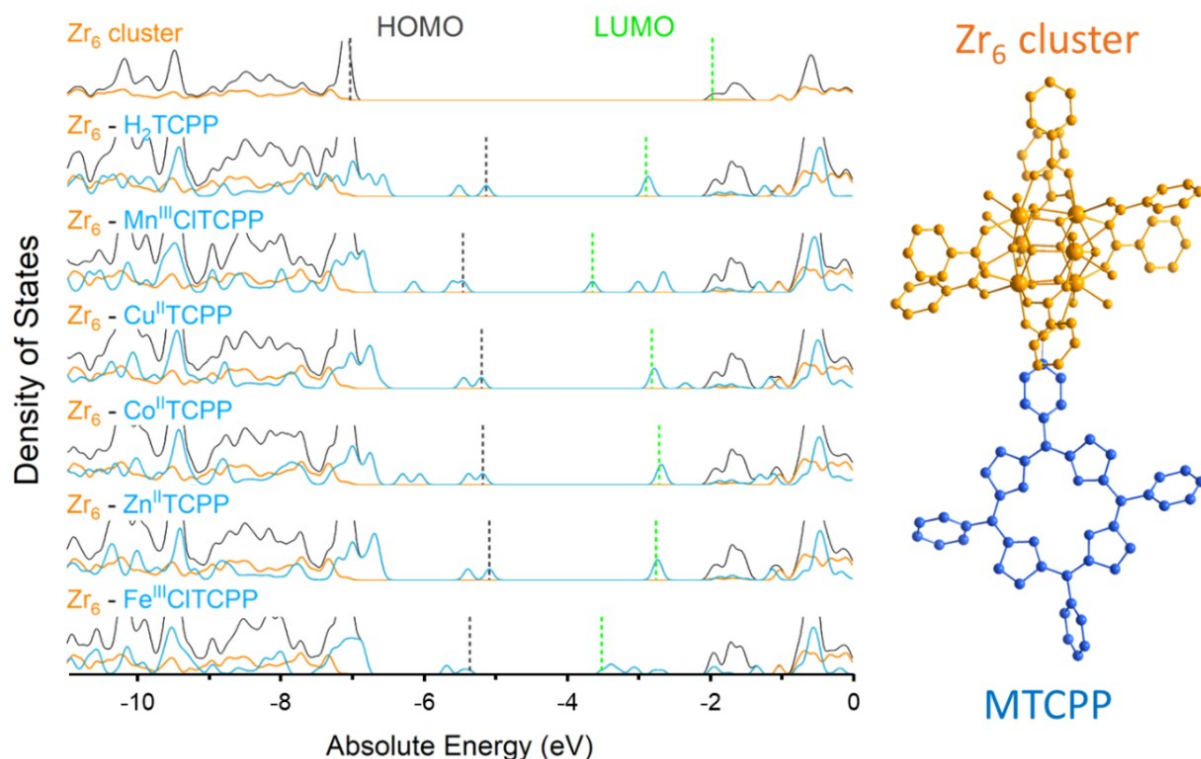


Figure S31. Density of States calculated for the Zr₆-oxo cluster, the MOF-545 and a series of MOF-545(TM) (from top to bottom), using cluster models consisting of a Zr₆ node and a TCPP linker, as represented on the right panel (H atoms omitted for clarity). The total DOSs are represented in black lines, whereas yellow and blue lines account for contribution from Zr atoms or from those belonging to the TCPP linker, respectively. Level of theory: HSE06/SDD,6-31g(d,p); IEF-PCM solvation model for acetonitrile.

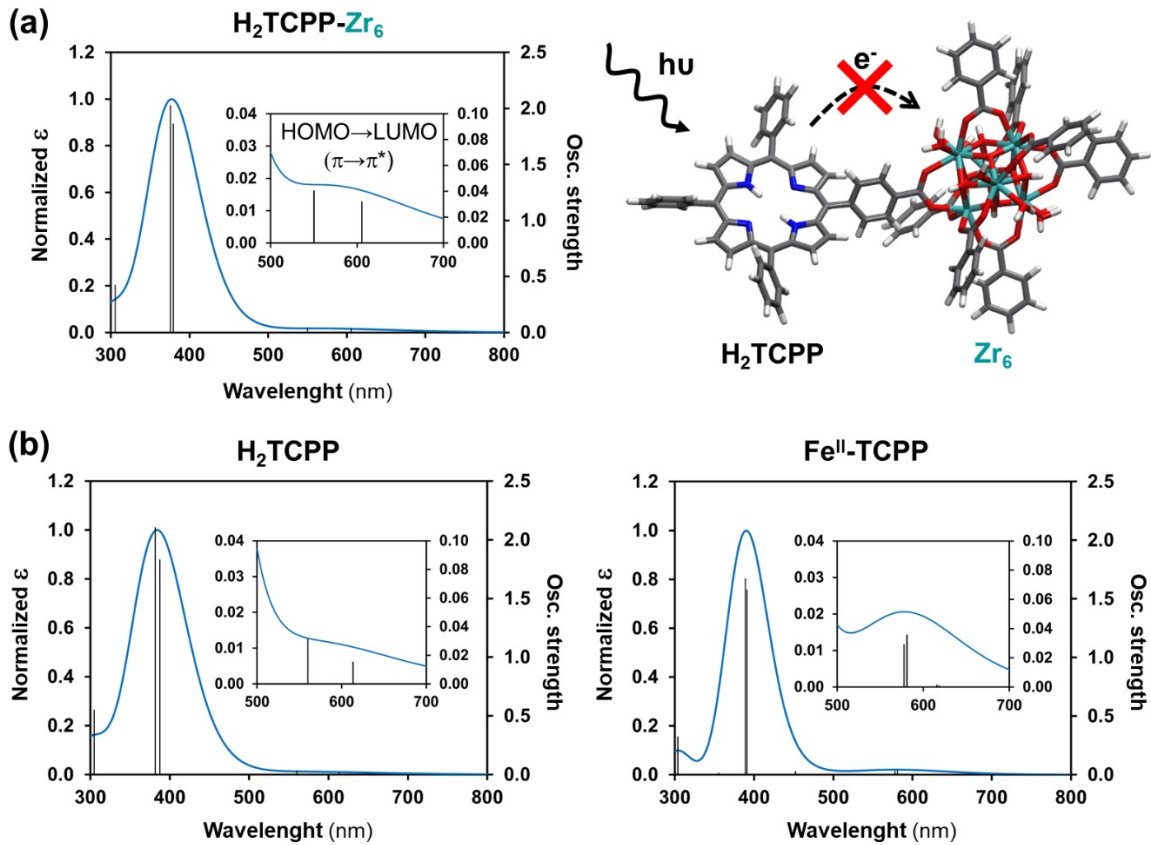


Figure S32. UV-Vis spectra obtained by means of TD-DFT (ω B97X-D/DZP level) for: a) the **H₂TCPP-Zr₆** model consisting of a Zr₆ cluster and one non-metallated linker of MOF-545 (represented in the right panel) and b) smaller models of the H₂TCPP and the Fe^{II}-TCPP linkers belonging to MOF-545 and the reduced form of MOF-545(Fe). The spectrum simulated for the large model reveals that the transitions in the visible region consist only in ligand-centred excitations that involve the frontier molecular orbitals of the porphyrin. As inferred from Figure S31, the lowest empty orbitals with d(Zr) contribution are much higher in energy and therefore, no charge transfer is expected to occur from the linker to the Zr₆ node of the MOF. Table S5 compiles a detailed analysis for the 6 less energetic excitations in the **H₂TCPP-Zr₆** model and does not show any excited state with charge-transfer character below in energy than those accessible in the visible range. The simulated spectra for isolated linkers (bottom) display the same features than that for the large model, further supporting that the Zr₆ node does not participate in the photo-activity of MOF-545 nor to that of its metallated derivatives.

Table S5. Analysis of the 6 first excited states obtained from time dependent DFT calculations (vertical excitations) for the $\text{H}_2\text{TCPP-Zr}_6$ system represented in Figure S33.

Excited State	Wavelength (nm)	Oscillator Strength	Main MO contributions ^a
1	605	0.0319	HOMO-1 → LUMO+1 (36.6 %) HOMO → LUMO (61.4 %)
2	550	0.0404	HOMO-1 → LUMO (41.3 %) HOMO → LUMO+1 (58.7 %)
3	379	1.8591	HOMO-1 → LUMO+1 (60.6 %) HOMO → LUMO (34.3 %)
4	375	2.0224	HOMO-1 → LUMO (57.3 %) HOMO → LUMO+1 (40.5 %)
5	320	0.0021	HOMO-3 → LUMO+10 (5.2 %) HOMO-2 → LUMO (92.2 %)
6	305	0.4237	HOMO-3 → LUMO (81.0 %) HOMO-2 → LUMO+10 (6.0 %)

^a All the MO involved in these transitions are porphyrin-centred orbitals and therefore, all these excited states have $\pi \rightarrow \pi^*$ character.

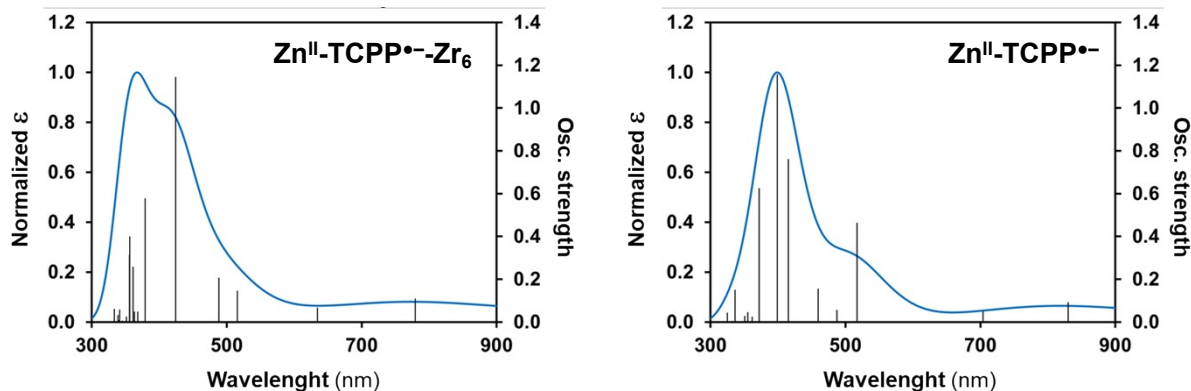


Figure S33. Simulated absorption spectrum for the one-electron reduced $\text{Zn}^{\text{II}}\text{-TCPP}^{\bullet-}\text{-Zr}_6$ model (left). For comparison, the spectrum of $\text{Zn}^{\text{II}}\text{-TCPP}^{\bullet-}$ is shown in the right panel. All the transitions in the visible range were found to involve linker-centred orbitals exclusively.

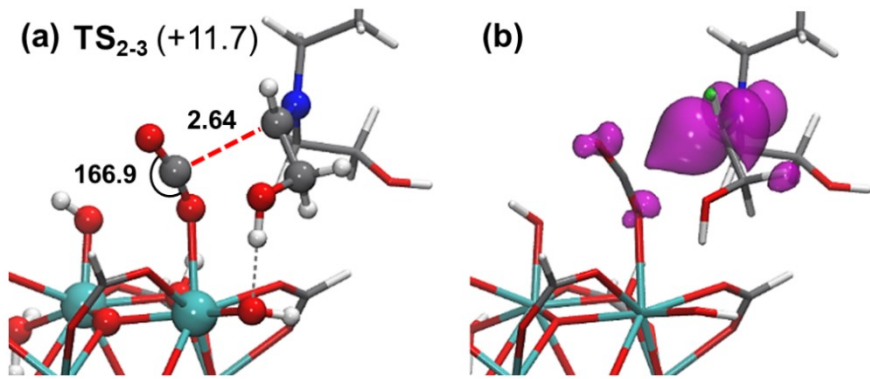


Figure S34. (a) Optimized geometry for TS_{2-3} . Relative energy with respect to the reactants is given in $\text{kcal}\cdot\text{mol}^{-1}$, and key geometrical parameters are given in Å and degrees. (b) Representation of the spin density distribution in the structure of TS_{2-3} .

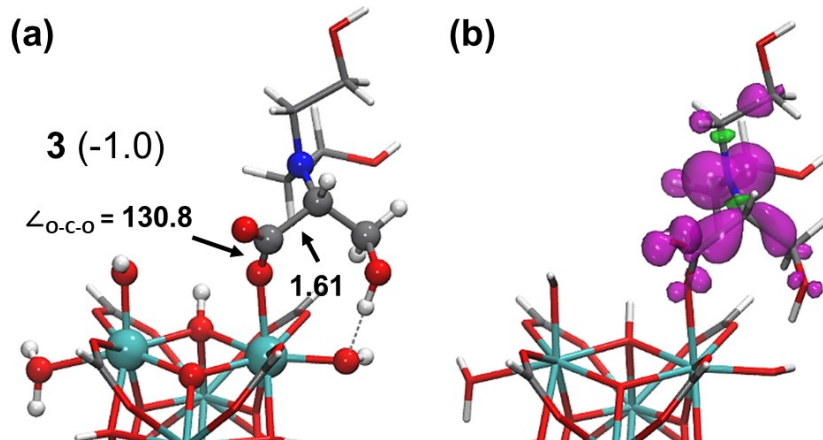


Figure S35. (a) Optimized geometry for species 3. Relative energy with respect to the reactants is given in $\text{kcal}\cdot\text{mol}^{-1}$, and key geometrical parameters are given in Å and degrees. (b) Representation of the spin density distribution in the structure of 3. The N atom is the centre supporting the highest spin density (0.66 e), in agreement with the zwitterionic nature of the complex where the radical cation is formally localized on the N atom.

Analysis of the key hydride-transfer step. The generation of intermediate **4** from the **2**-TEOA $^{\bullet}$ adduct occurs through TS_{2-4} , in which a formal hydride is transferred from the TEOA $^{\bullet}$ to the Zr^{IV}-bound CO₂ molecule. This process is followed by a spontaneous (and nearly barrierless) proton transfer from the transient, positively-charged organic molecule to the Zr₆ cluster of the MOF. The analysis of the spin density distribution in TS_{2-4} (Figure S36) reveals that the unpaired electron initially localized on the N and C atoms of TEOA $^{\bullet}$ is delocalized over the CO₂ and the TEOA fragments, typical of a proton-coupled electron-transfer (PCET) process.¹⁴ Thus, as schematically depicted in Scheme S1, the process from **2** to **4** should be described as a concerted asynchronous PCET and single electron transfer (SET) from the TEOA $^{\bullet}$ fragment to CO₂ (accounting for a formal hydride transfer), followed by a spontaneous proton migration. The intermediates involved in this process could not be characterized because they might represent transient species located on very shallow minima of the potential energy surface (see Figures S37, S38), which existence should depend on the experimental conditions.

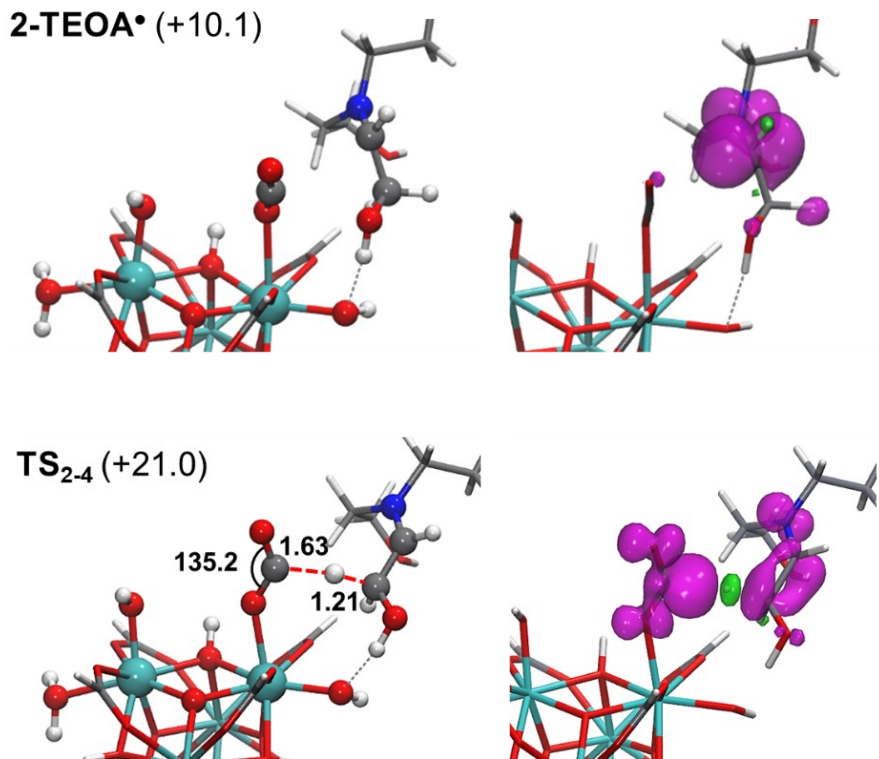


Figure S36. DFT-optimized structures of the **2-TEOA[•]** non-covalent adduct (top) and **TS₂₋₄**, (bottom) accompanied by their respective representations of the spin density distributions. Relative Gibbs free energies (kcal·mol⁻¹) with respect to the reactants are given in parenthesis.

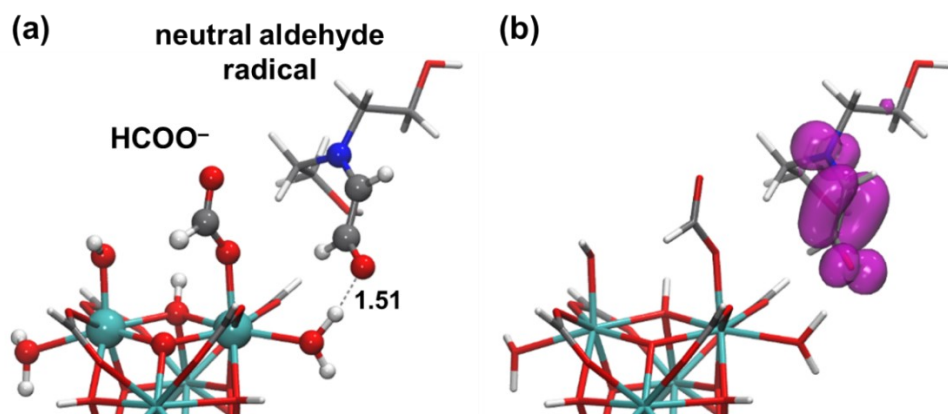


Figure S37. Optimized structure of the product generated after **TS₂₋₄**, corresponding to the hydrogen-bonded adduct between **4** and the neutral aldehyde radical derived from TEOA (distance in Å). The spin density distribution delocalized over the aldehyde-like fragment in the right panel confirms the nature of the complex.

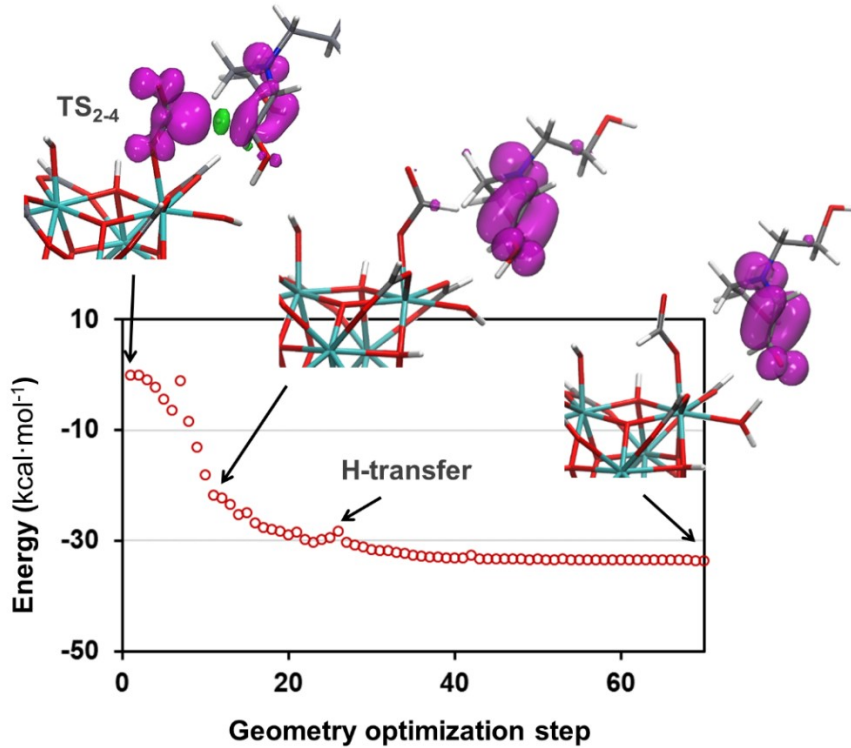
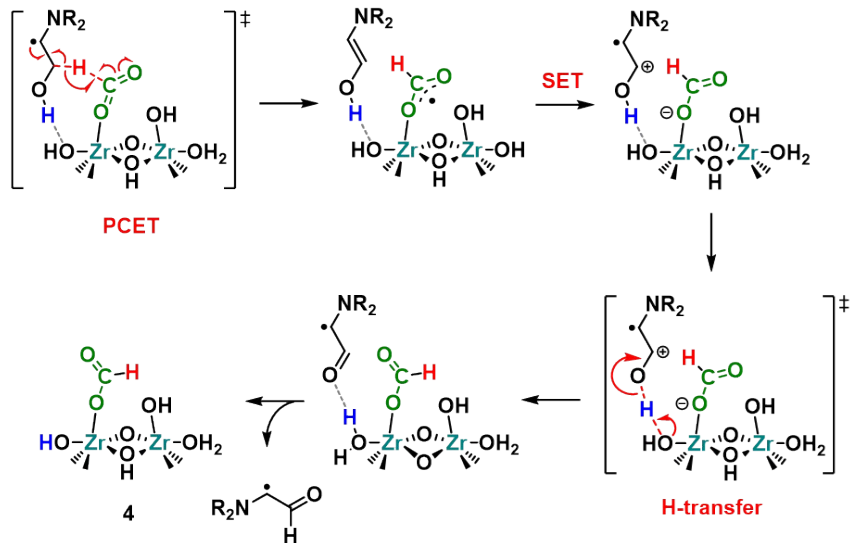


Figure S38. Geometry, energy and spin-density evolution along the geometry optimization from TS_{2-4} to products using the smallest geometry step size permitted in the Gaussian16 software. The localization of the spin density on the organic moiety along with its disappearance from the CO_2 molecule after a few geometry steps indicates a single-electron transfer process from the TEOA^\bullet molecule to CO_2 . The small hill that can be appreciated after 26 steps corresponds to the energy barrier for the spontaneous proton transfer from the positively charged enol radical to the Zr-OH site of the MOF, for which we can estimate a very low energy barrier of ca. $1.8 \text{ kcal}\cdot\text{mol}^{-1}$.

Scheme S1. Proposed pathway and transient intermediates involved in the formal hydride-transfer process from TEOA^\bullet to CO_2 .



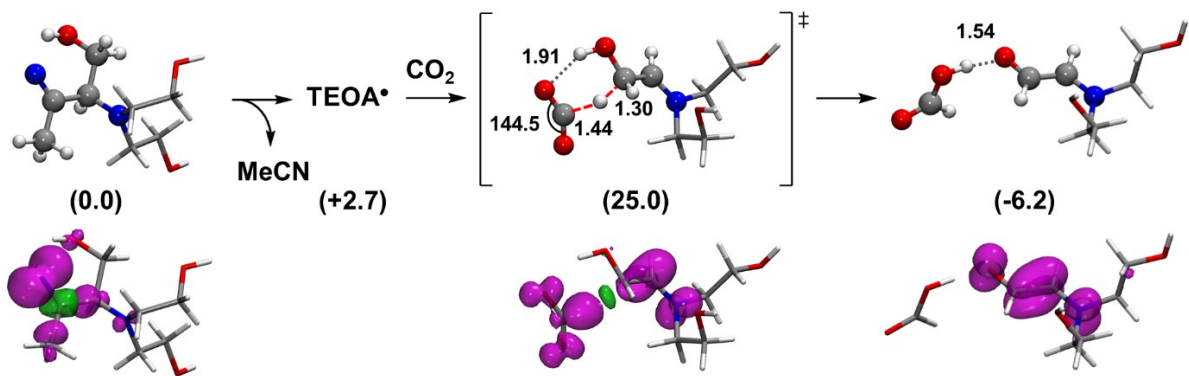


Figure S39. Hydrogenation of CO_2 promoted by TEOA^\bullet *without* the assistance of a Zr^{IV} center as Lewis acid. Relative Gibbs free energies in parentheses are given in $\text{kcal}\cdot\text{mol}^{-1}$ and relevant distances and angles are given in \AA and degrees, respectively. Magenta and green volumetric representations illustrate the distribution of the excess of alpha and beta spin density, respectively, for each species.

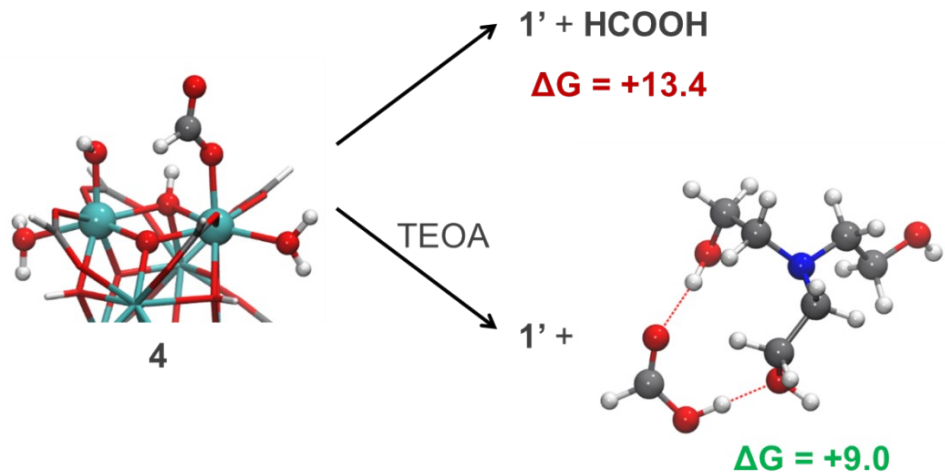
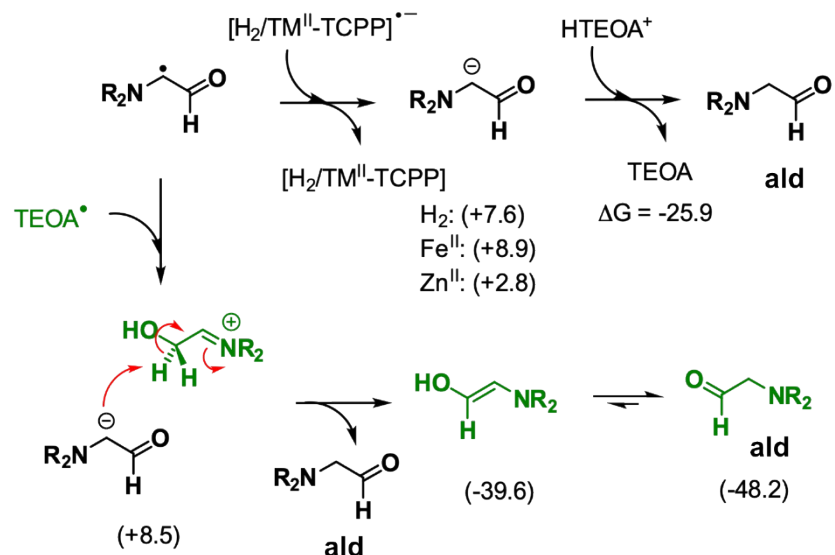


Figure S40. Free energy cost ($\text{kcal}\cdot\text{mol}^{-1}$) associated to the release of the HCOOH product from the Zr -oxo cluster, highlighting the role of TEOA of a stabilizing the product in solution via formation of a non-covalent adduct and consequently, reducing the energy cost of the decoordination.

Scheme S2. Possible termination routes after the CO₂ reduction step. Relative Gibbs free energies and reaction energies are given in kcal·mol⁻¹.



4. NMR and mass spectrometry experiments

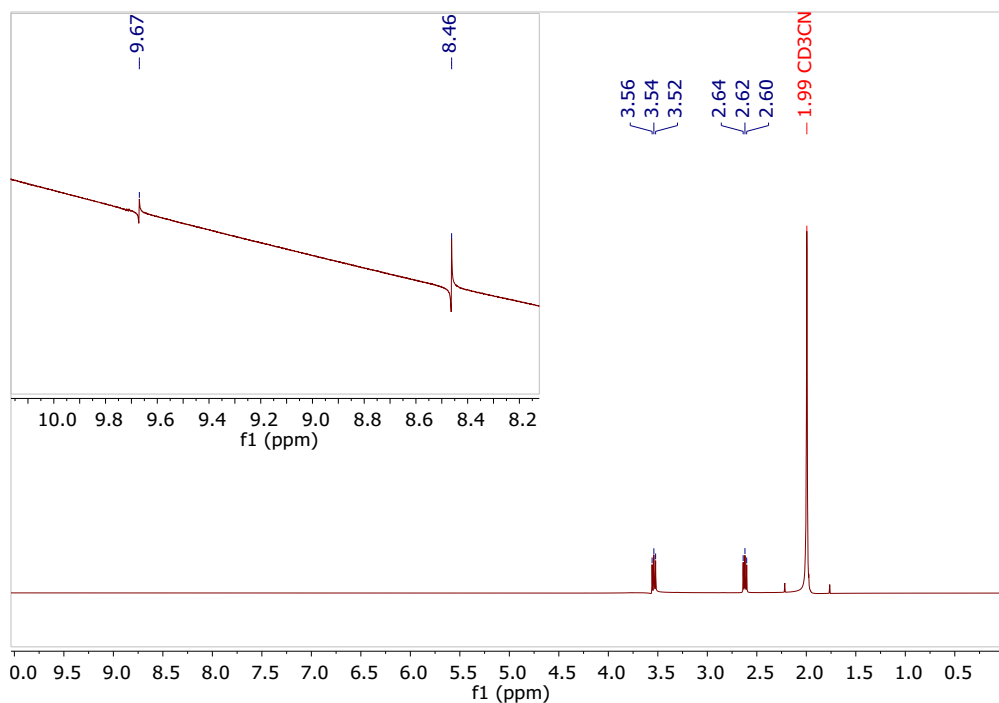


Figure S41. ¹H NMR spectrum of the reaction mixture after the catalysis. The triplets at 2.62 and 3.54 ppm are assigned to the alkyl protons in TEOA; whereas smaller peaks at 8.46 and 9.67 ppm are assigned to the C-bound proton of formic acid and the proton of the aldehyde function in the oxidized form of TEOA (labeled as **ald**), respectively.



Figure S42. HRMS spectrum of the reaction mixture after 4 h of photocatalytic experiments with NanoMOF-545(Fe) (see experimental section for details).

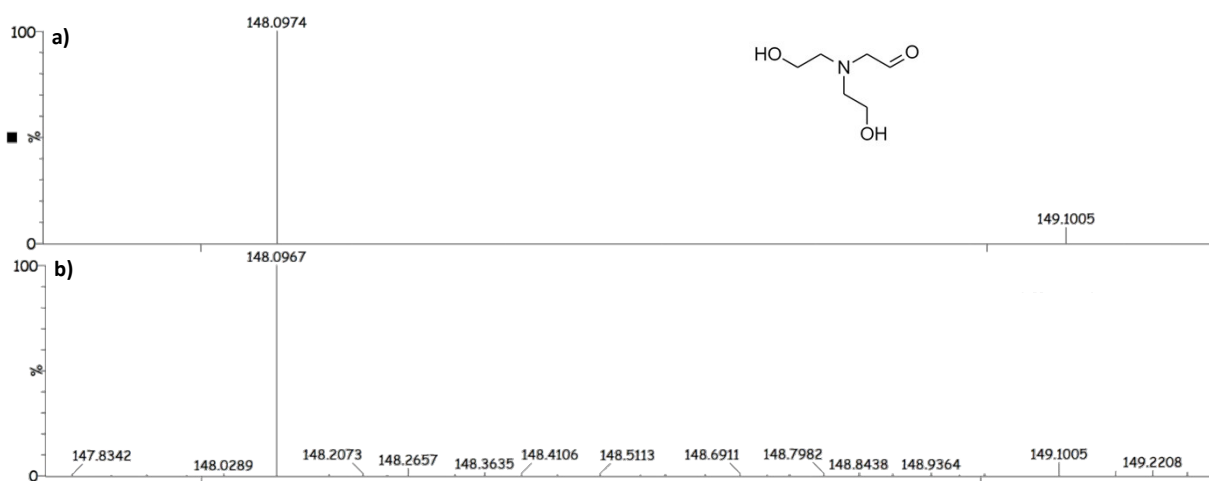


Figure S43. a) Expected HRMS spectrum for C₆H₁₃NO₃; b) experimental HRMS spectrum.

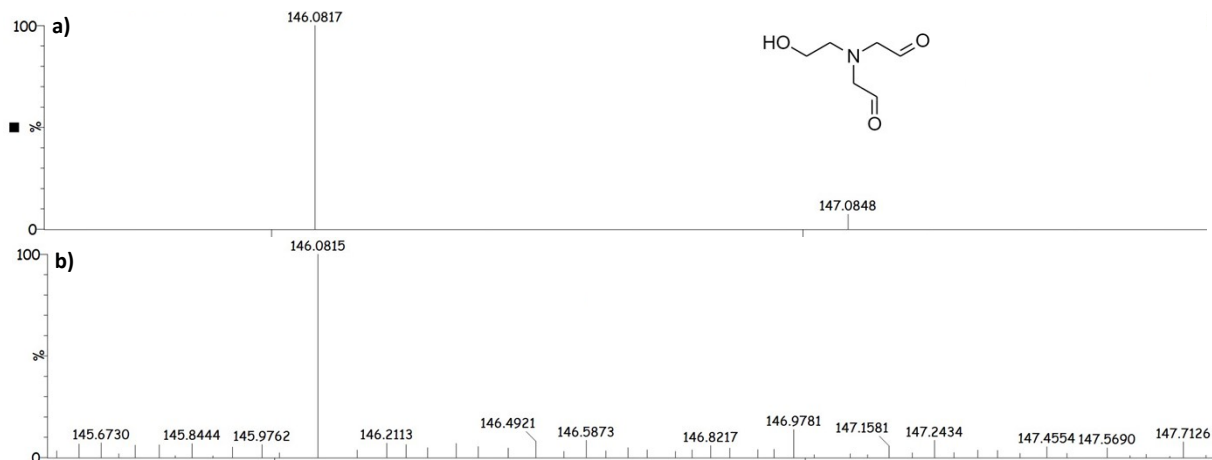


Figure S44. a) Expected HRMS spectrum for C₆H₁₁NO₃; b) experimental HRMS spectrum.

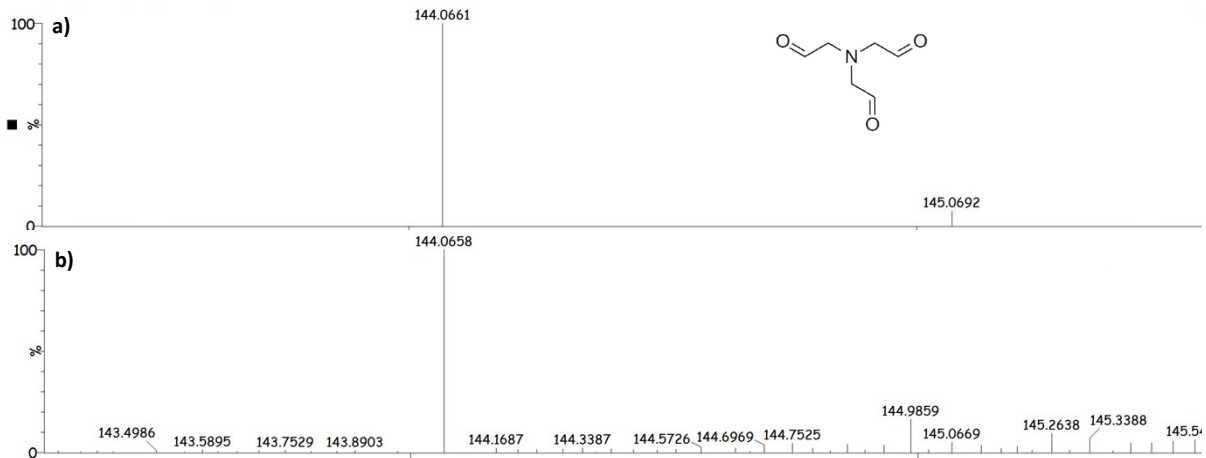


Figure S45. a) Expected HRMS spectrum for $\text{C}_6\text{H}_9\text{NO}_3$; b) experimental HRMS spectrum.

5. Additional computational results.

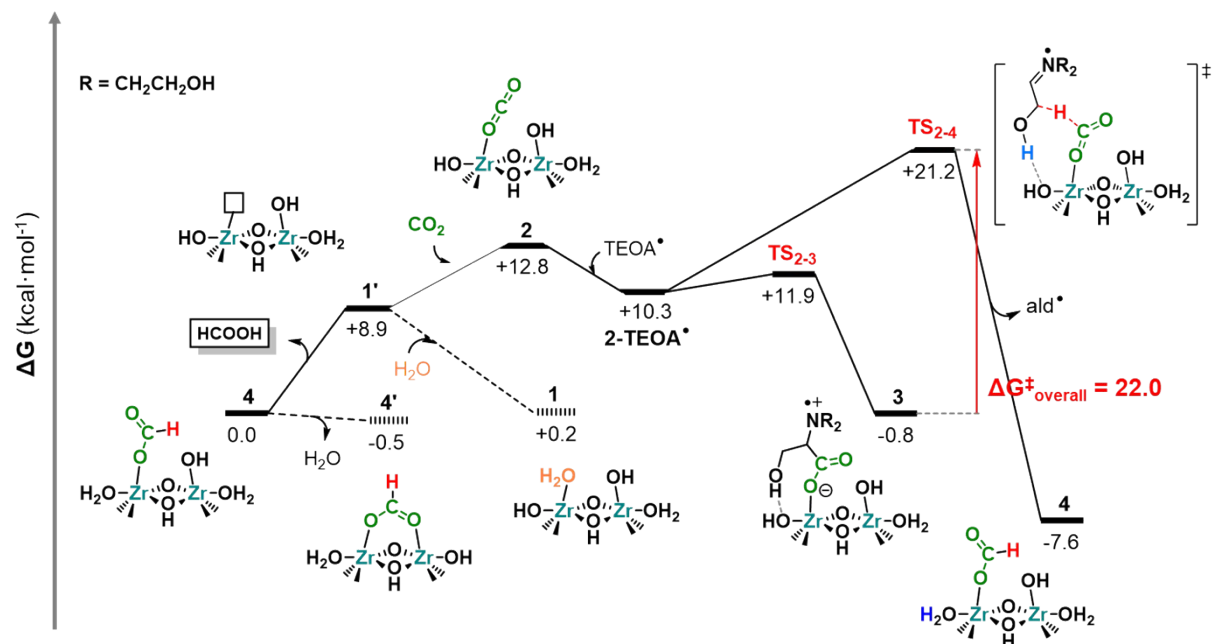


Figure S46. Calculated Gibbs free-energy profile (kcal mol⁻¹) for the reduction of CO_2 from species **4**, showing that the reduction of a second CO_2 molecule provides the thermodynamic driving force for the release of the product.

Alternative, less favourable mechanisms. We have evaluated whether TEOA^\bullet acting as a hydride donor could serve to generate a Zr-hydride from species **1'**. The resulting Zr-hydride intermediate and ald• byproduct are 3.5 kcal mol⁻¹ higher in energy than **TS₂₋₄**, suggesting that this pathway might not be operative. This is indeed consistent with the lack of H_2 product. A sequential electron transfer and proton transfer mechanism from **2** + TEOA^\bullet was also predicted to be unlikely, involving a one-electron reduced Zr-(OCO^\bullet) intermediate that lies 30.9 kcal mol⁻¹ above the reactants.

6. Use of DMPO radical scavenger in photocatalytic reduction of CO₂

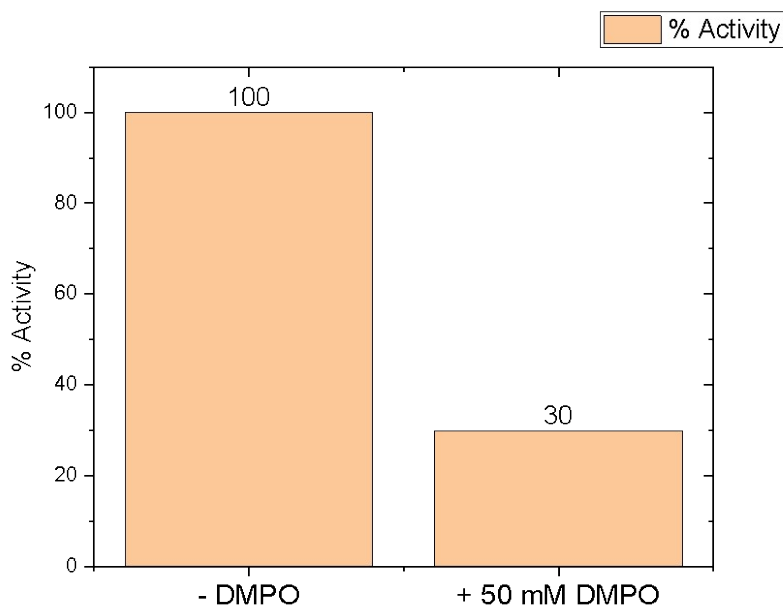


Figure S47. Use of DMPO radical scavenging in the photocatalytic reduction of CO₂ reduction with MOF-545(Fe). Normalized catalytic activity of the MOF-545(Fe) in the presence of 50 mM of the radical scavenger, 5,5-dimethyl-1-pyrroline-N-oxide (DMPO), after 1 h illumination. Reaction conditions: photocatalyst 1 mg, MeCN/TEOA (10:1) 1 mL ($\lambda > 415$ nm, 280 W).

7. UV-Vis Spectral Titrations of ZnTCPP with FeTCPPCl

Porphyrin Ligand titration protocol: For both ZnTCPP and FeTCPPCl titrations, stock solutions were first prepared in DMF (1.7×10^{-4} M ZnTCPP, 3.0×10^{-4} M FeTCPPCl). Aliquots from the stock solutions were then used to make the sample solutions. The porphyrin sample volume (0.5 mL) was kept constant, while the TEOA volume was incrementally increased for each sample (0 - 2 mL 0.01 M/0.1M TEOA for FeTCPPCl, 0 - 100 μ L pure TEOA for ZnTCPP). The porphyrin and TEOA mixtures were all diluted to a final sample volume of 3 mL and stirred 1 min before UV-Vis measurements.

Given that both (Zn)TCPP and (Fe)TCPPCl can be axially ligated,^{9,10} photoreduction of the porphyrin macrocycles are primarily driven by inner-sphere electron transfer via excitation of charge-transfer bands.^{11,12} Therefore, the enhanced photocatalytic behavior of metalated MOF-545 is rationalized by how readily the metalloporphyrin coordinates TEOA. UV-Vis titrations with TEOA in DMF solutions of (Zn)TCPP and (Fe)TCPPCl were performed to determine binding constants (Figures S48-S51). The change in absorbance ($OD_{[TEOA]} - OD_{initial}$, ΔOD) at certain wavelengths were plotted vs. [TEOA] and fitted to 1:1 and 1:2 binding models (non-linear regression) using the fitting software available at supramolecular.org/bindfit and from prior literature.¹³ (Zn)TCPP exhibited a 1:1 binding constant (K_{11}) of 5.4 ± 0.3 M⁻¹ and (Fe)TCPPCl had a K_{11} of $(15 \pm 3) \times 10^3$ M⁻¹ and a K_{12} of 48 ± 1 M⁻¹, which are in agreement with the catalytic trends of the MOFs.

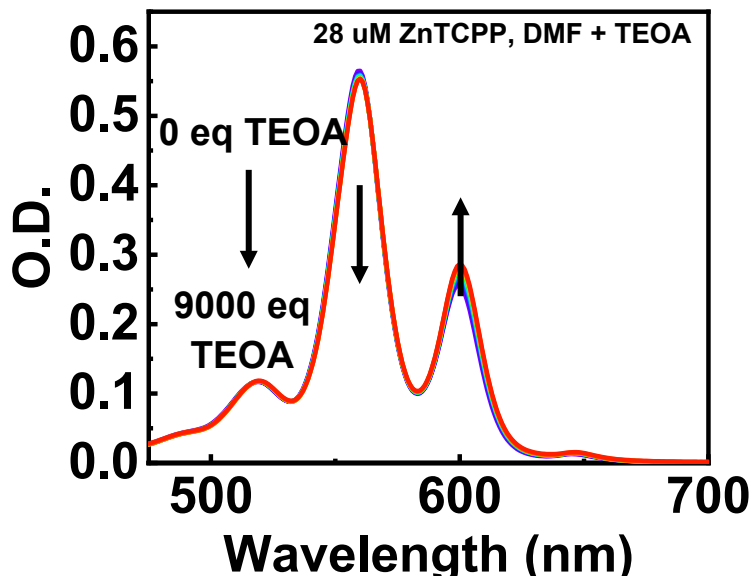


Figure S48. Steady-state electronic absorption spectra of 28 μM (Zn)TCPP in DMF with increasing equivalents of TEOA added.

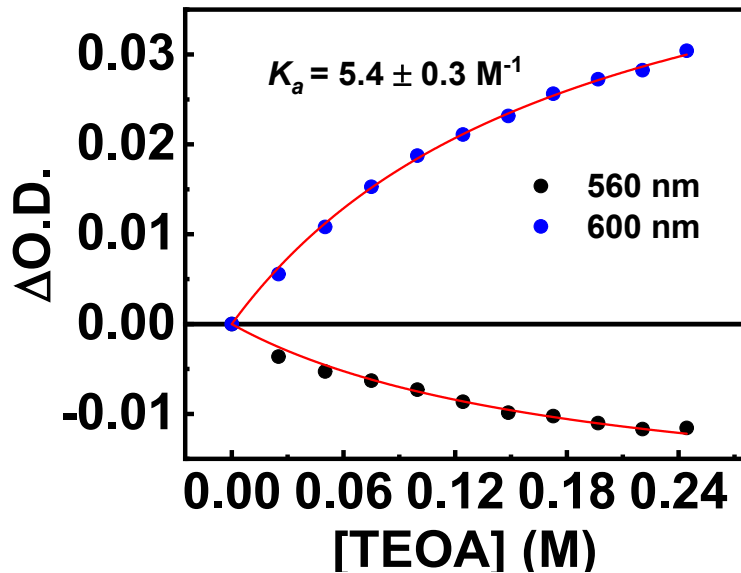


Figure S49. Absorbance change of (Zn)TCPP ($\text{OD}_{[\text{TEOA}]} - \text{OD}_{\text{initial}}$) with increasing [TEOA] at 560 and 600 nm. The association constant, K_a , was determined via global fitting the two wavelengths to a 1:1 binding model.¹³

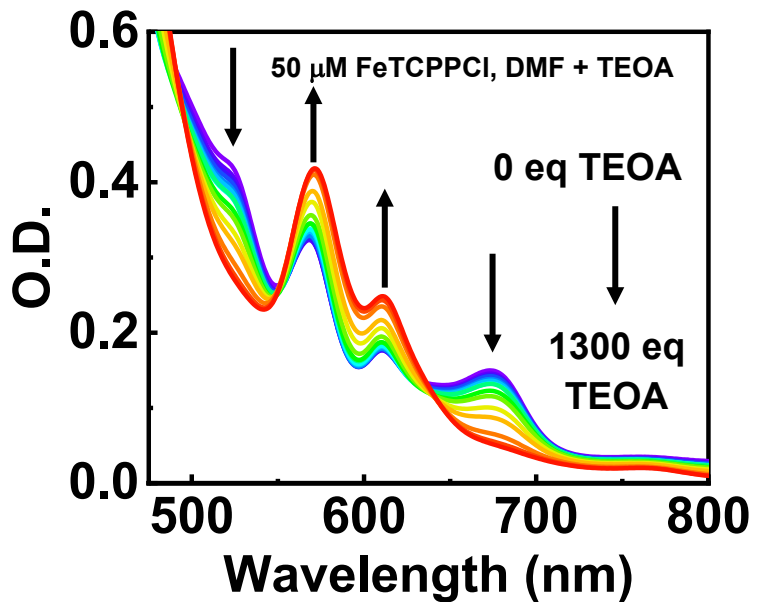


Figure S50. Steady-state electronic absorption spectra of 50 μM (Fe)TCPPCl in DMF with increasing equivalents of TEOA added.

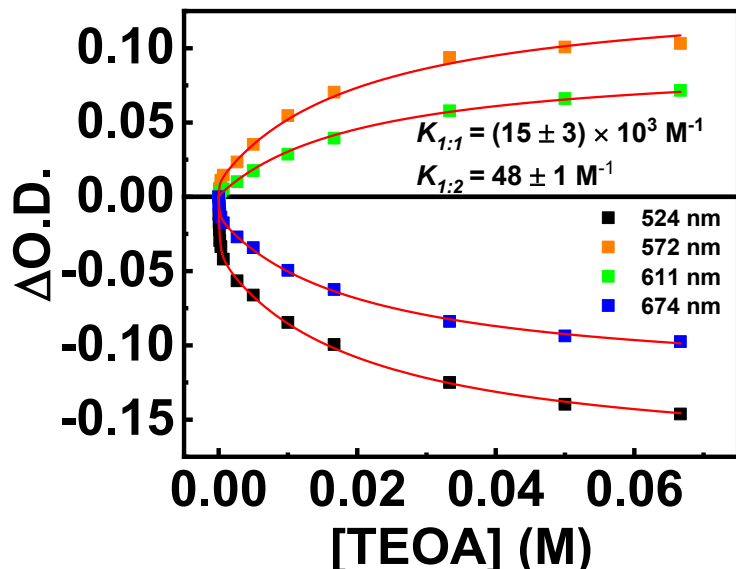


Figure S51. Absorbance change of (Fe)TCPPCl ($\text{OD}_{[\text{TEOA}]} - \text{OD}_{\text{initial}}$) with increasing $[\text{TEOA}]$ at 524 nm, 572 nm, 611 nm and 674 nm, globally fit to a binding model including 1:1 and 1:2 binding constants.¹³

8. References

- (1) Feng, D.; Gu, Z.-Y.; Li, J.-R.; Jiang, H.-L.; Wei, Z.; Zhou, H.-C. Zirconium-Metallocporphyrin PCN-222: Mesoporous Metal–Organic Frameworks with Ultrahigh Stability as Biomimetic Catalysts. *Angewandte Chemie International Edition* **2012**, *51* (41), 10307–10310.
- (2) Paille, G.; Gomez-Mingot, M.; Roch-Marchal, C.; Lassalle-Kaiser, B.; Mialane, P.; Fontecave, M.; Mellot-Draznieks, C.; Dolbecq, A. A Fully Noble Metal-Free Photosystem Based on Cobalt-Polyoxometalates Immobilized in a Porphyrinic Metal–Organic Framework for Water Oxidation. *J. Am. Chem. Soc.* **2018**, *140* (10), 3613–3618.
- (3) Bonnett, B. L.; Ilic, S.; Flint, K.; Cai, M.; Yang, X.; Cornell, H. D.; Taylor, A.; Morris, A. J. Mechanistic Investigations into and Control of Anisotropic Metal–Organic Framework Growth. *Inorg. Chem.* **2021**, *60* (14), 10439–10450.
- (4) Fidalgo-Marijuan, A.; Barandika, G.; Bazán, B.; Urtiaga, M.-K.; Arriortua, M.-I. Self-Assembly of Iron TCPP (Meso-Tetra(4-Carboxyphenyl)Porphyrin) into a Chiral 2D Coordination Polymer. *Polyhedron* **2011**, *30* (16), 2711–2716.
- (5) Shaikh, S. M.; Chakraborty, A.; Alatis, J.; Cai, M.; Danilov, E.; Morris, A. J. Light Harvesting and Energy Transfer in a Porphyrin-Based Metal Organic Framework. *Faraday Discuss.* **2019**, *216*, 174–190.
- (6) Jiang, H.-L.; Feng, D.; Wang, K.; Gu, Z.-Y.; Wei, Z.; Chen, Y.-P.; Zhou, H.-C. An Exceptionally Stable, Porphyrinic Zr Metal–Organic Framework Exhibiting PH-Dependent Fluorescence. *J. Am. Chem. Soc.* **2013**, *135* (37), 13934–13938.
- (7) Taniguchi, M.; Lindsey, J. S.; Bocian, D. F.; Holten, D. Comprehensive Review of Photophysical Parameters (ϵ , Φ_f , T_s) of Tetraphenylporphyrin (H₂TPP) and Zinc Tetraphenylporphyrin (ZnTPP) – Critical Benchmark Molecules in Photochemistry and Photosynthesis. *Journal of Photochemistry and Photobiology C: Photochemistry Reviews* **2021**, *46*, 100401.
- (8) Nappa, M.; Valentine, J. S. The Influence of Axial Ligands on Metallocporphyrin Visible Absorption Spectra. Complexes of Tetraphenylporphinatozinc. *J. Am. Chem. Soc.* **1978**, *100* (16), 5075–5080.
- (9) King, R. B. *Encyclopedia of Inorganic Chemistry*, 2nd ed.; J. Wiley & sons: Chichester, 2005.
- (10) Cole, S. J.; Curthoys, G. C.; Magnusson, E. A.; Phillips, J. N. Ligand Binding by Metallocporphyrins. III. Thermodynamic Functions for the Addition of Substituted Pyridines to Nickel(II) and Zinc(II) Porphyrins. *Inorg. Chem.* **1972**, *11* (5), 1024–1028.
- (11) Grodkowski, J.; Behar, D.; Neta, P.; Hambright, P. Iron Porphyrin-Catalyzed Reduction of CO₂. Photochemical and Radiation Chemical Studies. *J. Phys. Chem. A* **1997**, *101* (3), 248–254.
- (12) Dhanasekaran, T.; Grodkowski, J.; Neta, P.; Hambright, P.; Fujita, E. P-Terphenyl-Sensitized Photoreduction of CO₂ with Cobalt and Iron Porphyrins. Interaction between CO and Reduced Metallocporphyrins. *J. Phys. Chem. A* **1999**, *103* (38), 7742–7748.
- (13) Thordarson, P. Determining Association Constants from Titration Experiments in Supramolecular Chemistry. *Chemical Society Reviews* **2011**, *40* (3), 1305–1323.
- (14) Tantawy, W.; Hashem, A.; Yousif, N.; Flefel, E. The Water–Boryl Radical as a Proton-Coupled Electron Transfer Reagent for Carbon Dioxide, Formic Acid, and Formaldehyde — Theoretical Approach. *Can. J. Chem.* **2013**, *91* (2), 155–168.

9. Optimized Cartesian Coordinates (Å) and Gibbs Free Energies (a.u.) for the most representative structures obtained at the **o**B97X-D level

1

$\Delta G = -3006.905455$

O	1.94054893	3.33486130	1.31838365
C	3.13672013	2.97338153	1.15024366
O	3.54455926	1.93728567	0.56811499
Zr	2.47236592	0.06720755	-0.09970008
Zr	-0.07819026	2.37035619	0.75513349
C	3.42164040	-0.80993765	2.85280233
H	1.09157685	-4.59864891	0.15482595
O	2.08515589	-3.15490480	-1.58957956
O	3.71770688	-0.48598153	1.67346155
H	-0.84796611	-3.97761843	-2.92294051
C	-3.21704626	-3.05945987	-0.88695683
H	-0.38442381	-3.06020566	3.86932663
O	-1.84297146	-1.63940139	3.24721349
O	-3.59563587	-1.92402411	-0.49134798
H	0.87537230	0.14486198	4.67252021
C	-3.32408905	2.84135801	1.09850720
H	-1.09772523	3.19393284	-3.18804067
O	-2.24080986	1.43870070	-3.11208039
O	-3.66248584	1.67205655	0.77548166
H	0.55417815	-0.01602807	-4.74170294
C	3.13919025	1.03819153	-3.08314647
H	0.69256760	4.64576086	-0.33994576
O	3.55282247	0.73300480	-1.93120482
H	-0.91763047	4.00467889	2.89224742
C	-3.39224606	1.21860240	-2.67227224
O	-2.15729656	3.29947474	1.17835035
O	-3.70358240	0.56051507	-1.64052074
H	0.65255190	3.96806265	2.93425388
H	-0.19920088	3.55538324	-1.93666360
O	1.94619255	1.14100528	-3.45945814
C	3.25633678	-2.72131350	-1.46647777
H	1.17014993	-2.88635650	3.95758391
O	2.26958999	-0.99718430	3.32089511
O	3.62501975	-1.69992560	-0.82650673
C	-3.04493532	-1.49719527	2.91726964
O	-2.03771550	-3.43946330	-1.08043415
O	-3.49548193	-0.83853575	1.94060176
H	0.70068999	-3.80502662	-3.06222114
Zr	-2.48489333	-0.09628646	0.09654252
O	1.04068006	-0.63440060	-1.38413649
O	-1.31906902	0.84551600	1.93508769
O	-1.39858351	-0.93378383	-1.83871518
O	1.09634361	0.69508839	1.30460971
O	1.45847365	-1.81916482	0.86120680
O	-0.99933268	-1.37341104	0.67723855
O	-1.13405390	1.28981663	-0.59100945
O	1.30353609	1.84462154	-0.94597243
O	0.21353952	-4.22997956	0.02520437
Zr	0.02179604	-2.40795973	-0.77306814
O	-0.12998083	-3.33117447	-2.91664566
O	0.41519951	-2.88037352	3.35531543
Zr	0.14123399	-0.76843406	2.40443807
O	0.03544160	0.10386762	4.20466102
O	-0.21784854	3.05680462	-2.81143454
Zr	-0.08720427	0.78244646	-2.41191274
O	-0.27422075	0.03301823	-4.25419140
O	-0.09707566	4.09738769	-0.39107398
O	-0.14319444	3.43197541	2.81659844
H	2.06215171	-2.49955758	1.17270069
H	1.84696877	2.56115881	-1.28634523
H	-1.95314695	-1.25441644	-2.55641541
H	-1.82477853	1.14056306	2.69873371

H	3.91466039	1.24383132	-3.83516882
H	4.05307703	-3.30017960	-1.95640631
H	4.26423671	-0.95232622	3.54464463
H	-3.79395378	-1.99029404	3.55436810
H	-4.14365860	3.53310700	1.34175039
H	-4.23307839	1.63163794	-3.24973615
H	3.90950199	3.64733141	1.54740772
H	-4.01363739	-3.79094584	-1.08682185

1'

$\Delta G = -2930.495069$

O	-2.00523377	-1.41168025	3.17918532
C	-3.19299682	-1.24656158	2.78983447
O	-3.57807563	-0.90631543	1.64303676
Zr	-2.47244993	-0.07713444	-0.13784815
Zr	0.02950611	-1.14452346	2.12680550
C	-3.42673377	2.63677430	1.30152314
H	-0.85739806	3.58019848	-2.93250163
O	-1.88218218	1.06468393	-3.49196670
O	-3.72048651	1.58836947	0.66861698
C	3.25320345	1.44981095	-2.86826795
H	0.41349893	4.91139488	0.53177671
O	1.85857846	3.43239760	1.11395318
O	3.60969422	0.98385453	-1.75236047
H	-0.91100592	3.19326020	3.34593083
C	3.27236111	-1.27772413	2.74448456
H	1.03527406	-4.53012462	-0.07820835
O	2.18928843	-3.23432155	-1.28766943
O	3.62823594	-0.67393227	1.69676393
H	-0.58378816	-3.19102216	-3.51955802
C	-3.14897454	-2.86266879	-1.58133056
H	-0.76953245	-3.52712124	2.94135471
O	-3.55722024	-1.82495952	-0.99209534
H	0.85209306	-0.84739815	4.79806861
C	3.34732235	-2.79023337	-1.10598896
O	2.09934401	-1.53318497	3.11064037
O	3.67406607	-1.60816413	-0.80832968
H	-0.71873820	-0.77911176	4.79852388
H	0.13643889	-3.88134886	1.05255487
O	-1.95696415	-3.21484203	-1.75968708
C	-3.07667436	0.86720719	-3.15170415
H	-1.14431367	4.85244213	0.68268417
O	-2.27418943	3.07594502	1.54428071
O	-3.51458426	0.66270029	-1.98813521
C	3.05812724	3.08955587	0.98046988
O	2.08005476	1.56523175	-3.30103899
O	3.50063433	1.93157176	0.74712248
Zr	2.48693290	0.10983811	-0.03996376
O	-1.00229188	-0.48982143	-1.47376835
O	1.29618803	0.75275759	1.91627139
O	1.41478601	-0.63547054	-2.01437031
O	-1.11727981	0.44956386	1.32996104
O	-1.41770740	1.93387743	-0.76942713
O	1.02161547	1.44942849	-0.53886364
O	1.11146287	-1.33815022	0.42696380
O	-1.34074153	-1.95551918	0.53643978
O	-0.04681289	3.06539229	-2.94771181
Zr	0.04993112	1.18229333	-2.30705153
O	-0.38063881	4.42007418	0.27933242
Zr	-0.13905392	2.25127088	1.09945409
O	-0.06730762	2.89509751	2.99199294
O	0.16314329	-4.14483099	0.08011197
Zr	0.07030504	-2.24739422	-1.24060355
O	0.23633595	-2.86149608	-3.13900684
O	0.02547616	-3.17957193	2.52426196
O	0.08134079	-0.47777733	4.34724140

H	-2.02517249	2.63200748	-1.03035689
H	-1.89230657	-2.69769560	0.80005528
H	1.98482815	-0.91745808	-2.73641568
H	1.80156203	1.06701282	2.67242097
H	4.06149678	1.78756207	-3.53243659
H	3.81308500	3.88180313	1.09055685
H	4.08238819	-1.60925492	3.40993624
H	-3.98010504	-1.43306056	3.53452272
H	-3.92660630	-3.53293287	-1.97445933
H	-3.82560636	0.89050991	-3.95667334
H	-4.27181521	3.23414413	1.67216266
H	4.17683324	-3.50203969	-1.22972876

2

$$\Delta G = -3119.014574$$

O	-1.81555062	2.97494284	-2.22262586
C	-1.02401372	3.92343235	-1.97301266
O	0.06573143	3.86175434	-1.34830825
Zr	0.96875149	2.24274367	-0.07939539
Zr	-1.79286267	0.73048033	-1.68413277
C	-0.57303329	3.97655608	2.16308108
H	2.38347789	0.05679988	4.04557115
O	3.40993432	0.63362465	1.92189987
O	0.34763816	3.88096998	1.31153626
C	0.60961280	-3.85856480	2.18169071
H	-2.00425756	0.43059050	4.58488233
O	-2.75612924	-0.81247592	3.00502895
O	-0.36211960	-3.83084770	1.37685166
H	-3.53320747	2.55444451	2.15246590
C	-3.63285996	-2.00552180	-1.94407050
H	0.54159822	-1.41821651	-4.38471804
O	0.85852243	-2.80719609	-2.78708739
O	-3.00993028	-2.67475392	-1.07476768
H	3.90826311	-1.19409182	-2.25211275
C	3.18246514	1.94886090	-2.40722944
H	-1.61880587	1.51779693	-4.19995924
O	2.58915215	2.67203177	-1.56318012
H	-4.56581639	1.08510079	-2.07360955
C	0.10606087	-3.74064626	-2.41609718
O	-3.40121713	-0.82518783	-2.30255484
O	-0.59435447	-3.78569488	-1.36958167
H	-3.92144172	2.51632203	-2.00478918
H	-0.24393856	-0.08880218	-4.03820902
O	2.92669773	0.75249462	-2.69661822
C	3.62600398	1.83348428	1.62335233
H	-1.47454693	1.90198066	4.48678516
O	-1.35980405	3.06742835	2.53271469
O	2.82173461	2.64118808	1.08227195
C	-3.04445552	-1.99930160	2.71626782
O	1.41024889	-2.92719429	2.43361861
O	-2.73512212	-2.62628272	1.66708866
Zr	-1.19292149	-2.22065056	0.10907174
O	1.67488350	0.32735928	-0.10956073
O	-2.57675360	-0.29541345	0.20703791
O	1.15931275	-2.10692823	-0.09173182
O	-0.99629252	1.63603484	0.05811991
O	0.61631594	1.25822652	2.04324191
O	-0.47353263	-0.93095920	1.53891286
O	-0.68488948	-0.94340790	-1.41278141
O	0.36313525	1.25898560	-2.05345743
O	1.91287743	-0.69731417	3.67909831
Zr	1.54136707	-0.75378563	1.72271373
O	-1.34130016	0.99952565	4.16987536
Zr	-1.63876175	0.86501743	1.86308873
O	-3.49017621	1.61334359	1.95623865
O	0.66441418	-0.52478590	-4.03853930

Zr	1.42365190	-0.76119259	-1.85995119
O	3.20442598	-1.70647456	-1.84097297
O	-1.66356379	0.66742729	-3.75063822
O	-3.92187842	1.63462853	-1.60821617
H	0.93574715	1.76837354	2.79339170
H	0.53915029	1.78346308	-2.84000887
H	1.63898447	-2.93841165	-0.15873161
H	-3.52553692	-0.41785468	0.31268375
O	3.72706015	-1.93986211	1.11002046
C	4.57965144	-1.41004305	0.50150919
O	5.46379209	-0.90727950	-0.05026704
H	0.76839597	-4.80779705	2.71277836
H	-3.64415049	-2.55426219	3.45239375
H	-4.47511892	-2.51544949	-2.43299875
H	-1.31239424	4.91335888	-2.35412297
H	4.01009886	2.42126528	-2.95491422
H	4.61988578	2.23373359	1.87098666
H	-0.69539345	4.95876986	2.64112730
H	0.05733337	-4.62441701	-3.06896915

2-TEOA•

$\Delta G = -3636.107889$

O	4.98784097	-0.75599490	-0.74845164
C	4.99300850	-2.00768201	-0.59932918
O	3.99790886	-2.75954062	-0.44190066
Zr	1.84073882	-2.31075622	0.03104858
Zr	3.29646215	0.81252997	-0.76815915
C	2.99611292	-2.72284671	3.01312266
H	-2.58083029	-0.40175256	2.90481096
O	-1.58669206	-2.94389797	0.62994518
O	2.73191018	-3.19577851	1.87798680
C	-2.80315206	2.18848772	0.90561726
H	0.57421144	0.64750744	4.86788317
O	0.95041037	2.18266411	3.47321477
O	-1.85118236	2.90717196	0.50377035
H	3.95873730	0.31702721	3.78264195
C	2.83124720	4.07534931	-0.95732671
H	1.52201509	1.05900844	-4.53043632
O	-0.22160077	1.73486372	-3.50034545
O	1.63480651	4.06031997	-0.56043384
H	-1.40936530	-1.61866191	-3.68198408
C	1.19492678	-3.39717524	-2.93248436
H	4.73184944	0.34690156	-2.93807447
O	1.69054135	-3.59961650	-1.79153364
H	5.45788805	2.46792951	-0.04226490
C	-0.51182955	2.88345952	-3.09249229
O	3.59706314	3.08997760	-1.08896300
O	-0.54487669	3.28336100	-1.89549829
H	5.95398807	0.98362286	0.10047640
H	2.74608095	0.58234485	-3.64591803
O	0.70779231	-2.32532455	-3.37107501
C	-0.83419071	-3.94459204	0.56915190
H	1.19208536	-0.78988712	4.96491087
O	2.74733664	-1.56162622	3.42782967
O	0.42768657	-3.94729481	0.53673898
C	0.50094089	3.27260253	3.04540324
O	-2.78795499	0.93864666	1.05771509
O	0.34618394	3.61322857	1.84052359
Zr	0.26050666	2.40640637	-0.02257984
O	0.16460285	-1.39187602	-0.69785818
O	2.35114548	1.92337891	1.00051993
O	-1.10057612	0.73562596	-1.01868894
O	2.64717084	-0.54363528	0.72500395
O	0.54471045	-1.52978615	1.84435721
O	0.03790860	0.84355234	1.29200840
O	1.39092934	1.26502485	-1.29490047

O	2.41266993	-1.00050580	-1.76304365
O	-2.17407632	-1.16553864	2.48082762
Zr	-1.20304990	-0.67033559	0.75710290
O	0.68363274	-0.19323104	4.40134317
Zr	1.80114109	0.29109006	2.41553171
O	3.41503296	0.99178041	3.36412187
O	1.88017972	0.28850220	-4.07041421
Zr	0.34938446	-0.25880713	-2.42929324
O	-1.34608283	-0.70540226	-3.38545780
O	4.02594193	0.95789314	-2.70296808
O	5.21804958	1.58644786	0.27222797
H	0.29256909	-2.15860591	2.52821127
H	2.96779338	-1.42946056	-2.42073425
H	-1.91855778	1.01241315	-1.44383201
H	2.83308622	2.64656607	1.41384500
H	-4.78276015	-0.28484353	1.49122465
O	-3.14918954	-1.21413515	-0.72168410
C	-3.63414082	-2.26310080	-0.94416914
O	-4.06578047	-3.27958280	-1.28803370
C	-5.36732588	-1.21073774	1.52675148
C	-6.27367215	-1.29730247	0.33620515
H	-5.96790803	-1.17258868	2.45520185
O	-4.50766342	-2.34568780	1.57192786
N	-6.71114044	-0.14873418	-0.30470521
H	-7.00129716	-2.10665775	0.33064081
H	-3.67199540	-2.06019652	1.99155593
C	-5.77886253	0.87029425	-0.75441280
C	-8.03430158	-0.14900195	-0.89485089
H	-4.78877674	0.63182287	-0.36572770
H	-5.70749440	0.85803156	-1.85317475
C	-6.15124524	2.27739910	-0.31882992
H	-8.06419581	0.55713927	-1.73116531
H	-8.27479216	-1.13996108	-1.30210394
C	-9.09383196	0.24285352	0.13016354
H	-7.15671324	2.53641457	-0.67996227
H	-5.44396059	2.97860989	-0.78618783
O	-6.08769725	2.34669738	1.09472130
H	-8.85323645	1.23768878	0.53311094
H	-9.05634838	-0.46890768	0.96820976
O	-10.34940458	0.22299770	-0.51850717
H	-6.38836835	3.21888406	1.36498527
H	-11.02267272	0.44963647	0.12823750
H	-1.32162480	-4.93005365	0.55450274
H	1.19724869	-4.25502734	-3.62011713
H	3.49307213	-3.40209984	3.72025742
H	5.97687764	-2.49762322	-0.62148774
H	0.21999983	4.02249476	3.79915816
H	3.24529269	5.06237776	-1.20792957
H	-3.75352372	2.68964099	1.13862764
H	-0.77924804	3.62882944	-3.85582076

TS₂₋₃

ΔG = -3636.105275

O	4.92781982	-0.83977294	-0.89476074
C	4.91525618	-2.09080239	-0.73720448
O	3.91331167	-2.82267325	-0.54030658
Zr	1.77455662	-2.33613712	0.00805632
Zr	3.26609298	0.75328527	-0.86483879
C	3.03634582	-2.75273398	2.94952061
H	-2.45341593	-0.28193125	3.04916007
O	-1.63309552	-2.89285875	0.77235707
O	2.71839419	-3.22618150	1.82884052
C	-2.71997094	2.28982858	1.03466343
H	0.76306307	0.66054546	4.88097763
O	1.11380200	2.18784741	3.45627230
O	-1.77901891	2.98112421	0.56483526

H	4.09634659	0.26777484	3.64497193
C	2.85678976	4.03133189	-1.05392189
H	1.36212464	1.00053392	-4.56729998
O	-0.33278195	1.72114335	-3.47535396
O	1.67683533	4.04486393	-0.60891286
H	-1.59324050	-1.61181008	-3.57167145
C	1.00820085	-3.43243595	-2.91715294
H	4.61358514	0.25296520	-3.08199950
O	1.54379129	-3.63611091	-1.79409558
H	5.47107552	2.38261658	-0.23929416
C	-0.57020882	2.88301199	-3.06966284
O	3.59413642	3.02862757	-1.21371492
O	-0.54130564	3.29738023	-1.87811137
H	5.95738603	0.89479339	-0.09674397
H	2.60631392	0.51196200	-3.71768557
O	0.52218135	-2.35576717	-3.34439811
C	-0.90822621	-3.91062918	0.67855512
H	1.35304526	-0.79011845	4.94392358
O	2.82887033	-1.58377433	3.36519303
O	0.34973934	-3.94512769	0.57155715
C	0.67094997	3.28520779	3.03984193
O	-2.72298854	1.04369415	1.20632959
O	0.47493186	3.62205408	1.84070484
Zr	0.29861678	2.41266072	-0.02044739
O	0.09121701	-1.39020098	-0.66441155
O	2.41058275	1.89402305	0.92720354
O	-1.13684493	0.76712853	-0.95162962
O	2.64347485	-0.58107496	0.65847318
O	0.56688881	-1.51711745	1.86250674
O	0.09171550	0.86181753	1.30936501
O	1.35338244	1.24024711	-1.32743733
O	2.30805753	-1.04925728	-1.81372370
O	-2.11624171	-1.06990573	2.60855371
Zr	-1.20599979	-0.62911185	0.83506820
O	0.83455455	-0.17897534	4.40551689
Zr	1.88029978	0.27975753	2.37423750
O	3.54939034	0.95221205	3.24700899
O	1.72090062	0.22949609	-4.10885959
Zr	0.23802916	-0.27095611	-2.40927094
O	-1.49804601	-0.69320281	-3.30089620
O	3.92374528	0.87423623	-2.82700259
O	5.23566042	1.50787889	0.09728121
H	0.32580656	-2.13522388	2.55992683
H	2.82750050	-1.49512301	-2.48910359
H	-1.96399736	1.05623884	-1.34986759
H	2.92537773	2.60702507	1.31795724
H	-4.69845847	-0.10446451	1.64605398
O	-3.20612531	-1.12355590	-0.52409947
C	-3.82033851	-2.11830615	-0.71136300
O	-4.22686041	-3.14798698	-1.06461565
C	-5.32380322	-1.00287611	1.65860530
C	-6.04450284	-1.16074151	0.34874540
H	-6.06441350	-0.86402987	2.46714399
O	-4.54714646	-2.16142373	1.92077536
N	-6.50227111	-0.05822884	-0.34280807
H	-6.70210188	-2.02527522	0.27146217
H	-3.66864934	-1.86778898	2.23610111
C	-5.64167089	1.07772971	-0.62845943
C	-7.74839537	-0.16301800	-1.07722763
H	-4.64925301	0.86538665	-0.23242500
H	-5.54028958	1.19316459	-1.71675891
C	-6.13194107	2.39357102	-0.04874865
H	-7.76569454	0.58932359	-1.87170450
H	-7.82826774	-1.14660327	-1.55808957
C	-8.95150699	0.04625606	-0.16233906
H	-7.15975109	2.59704266	-0.38174504
H	-5.49318047	3.19910865	-0.44057040

O	-6.05610574	2.31698963	1.36291534
H	-8.87835184	1.03662683	0.31076578
H	-8.92453758	-0.70458632	0.64119421
O	-10.11455799	-0.07594878	-0.95466377
H	-6.42520745	3.12581530	1.72815314
H	-10.87836836	0.04093128	-0.38375205
H	-1.41788864	-4.88468623	0.70373004
H	0.97059258	-4.29487785	-3.59797239
H	3.54534497	-3.43831767	3.64188676
H	5.88910078	-2.59828567	-0.79032333
H	0.43733471	4.04484925	3.80002387
H	3.28239919	5.00829685	-1.32394708
H	-3.64378986	2.81719379	1.31353051
H	-0.84544639	3.62744906	-3.83122853

3

$\Delta G = -3636.125622$

O	4.76213084	-1.22320556	-1.06435992
C	4.61789219	-2.46929789	-0.93782613
O	3.54976188	-3.09435481	-0.72306117
Zr	1.49518402	-2.41191922	-0.09430848
Zr	3.27638110	0.53570565	-0.92338550
C	2.81269815	-3.07032896	2.76947019
H	-2.37089715	0.02001256	3.15625785
O	-1.88634274	-2.69229064	0.91998285
O	2.41729113	-3.47076616	1.64430778
C	-2.41509349	2.69287202	1.29171603
H	1.00570790	0.47842718	4.91327746
O	1.39930322	2.02158378	3.52319276
O	-1.42639025	3.26521591	0.75766401
H	4.15531680	-0.20420164	3.54196798
C	3.22070408	3.83725827	-1.00362825
H	1.27807107	1.12075061	-4.52056879
O	-0.24254128	2.00261004	-3.36781435
O	2.06460642	3.96032165	-0.51973339
H	-1.88479897	-1.15720365	-3.55347463
C	0.51910264	-3.31345234	-3.01822616
H	4.48241115	-0.04617612	-3.19912601
O	1.08691946	-3.60877161	-1.93167260
H	5.65900589	1.89875912	-0.32540545
C	-0.35397794	3.16340502	-2.91029419
O	3.84505547	2.76849122	-1.21700872
O	-0.26519396	3.52326922	-1.70397573
H	5.99255446	0.36530438	-0.24876719
H	2.49769008	0.46106832	-3.75851253
O	0.12615023	-2.18005884	-3.38873358
C	-1.26992221	-3.76108562	0.73085219
H	1.45482339	-1.02258791	4.87638680
O	2.73168410	-1.90418089	3.23275110
O	-0.040000801	-3.90087032	0.46891438
C	1.09334351	3.18148130	3.15674005
O	-2.58244514	1.46141964	1.44855606
O	0.92276601	3.58606549	1.97529539
Zr	0.52638833	2.46194701	0.08541609
O	-0.10901311	-1.28108994	-0.68146515
O	2.60470191	1.69486158	0.93180916
O	-1.08681242	1.03609567	-0.85036067
O	2.56864124	-0.77846484	0.57578484
O	0.44612023	-1.53678404	1.81661013
O	0.19446228	0.89981638	1.35057692
O	1.42024793	1.23972286	-1.30804120
O	2.10371205	-1.12178151	-1.89223538
O	-2.12952686	-0.80336687	2.71788858
Zr	-1.30898940	-0.45321329	0.86701719
O	0.94700287	-0.34603895	4.41029918
Zr	1.92716321	0.09458892	2.33317895

O	3.68263264	0.55809039	3.19351180
O	1.57542906	0.28967025	-4.12645098
Zr	0.11136538	-0.10261747	-2.37697363
O	-1.64922820	-0.25622750	-3.31020629
O	3.88462448	0.64916639	-2.90586594
O	5.34882378	1.04260063	-0.00176615
H	0.16787315	-2.14435138	2.50874810
H	2.54746380	-1.59860639	-2.59926316
H	-1.90687254	1.39010499	-1.20857533
H	3.20088629	2.33653073	1.32981068
H	-4.61727605	0.18047339	1.83851683
O	-3.16471146	-0.63204151	-0.24030913
C	-4.10577776	-1.45054740	-0.47273808
O	-4.14849641	-2.42576051	-1.19416364
C	-5.21658241	-0.73124651	1.76307417
C	-5.48607177	-1.05764958	0.26425515
H	-6.19609921	-0.54537583	2.21593319
O	-4.59672725	-1.81435956	2.37763683
N	-6.05616606	-0.00283895	-0.47770585
H	-6.12790493	-1.93537453	0.18612681
H	-3.64590360	-1.57875417	2.49694810
C	-5.45364040	1.32314998	-0.51465037
C	-7.23274431	-0.26693324	-1.28066547
H	-4.53282401	1.29927441	0.06503717
H	-5.20737573	1.55180734	-1.55797544
C	-6.40445963	2.38494658	0.02494537
H	-7.34921236	0.52459373	-2.02227057
H	-7.08809292	-1.21988424	-1.80029276
C	-8.49234365	-0.35026976	-0.40543449
H	-7.28912312	2.47217087	-0.61994234
H	-5.87188268	3.34357362	-0.00783718
O	-6.75292808	2.00779788	1.33835454
H	-8.61780438	0.59247228	0.14158808
H	-8.37000935	-1.15313310	0.33507131
O	-9.55084193	-0.60815324	-1.29395721
H	-7.35252078	2.66803756	1.69771991
H	-10.36656744	-0.63979541	-0.78653785
H	-1.85039051	-4.69242156	0.81124390
H	0.35998570	-4.14487567	-3.72037205
H	3.27569729	-3.82720351	3.41936684
H	5.52859767	-3.07758197	-1.03793115
H	0.97119596	3.93481944	3.94927724
H	3.73972110	4.77186010	-1.26232616
H	-3.22068826	3.35374721	1.64679235
H	-0.56294331	3.96428359	-3.63591756

TS₂₋₄

$\Delta G = -3636.090572$

O	5.11477574	-0.67366640	0.05524035
C	5.11607410	-1.93251985	0.12387983
O	4.12790439	-2.70306458	0.02684447
Zr	1.90528897	-2.31048518	0.08154966
Zr	3.42061963	0.87811227	-0.21544298
C	2.45207300	-2.89797747	3.20275949
H	-2.65488658	-0.50780748	2.38595963
O	-1.57687339	-3.07710355	0.10864354
O	2.45066612	-3.30564359	2.01263487
C	-2.93090357	2.09371328	0.28893952
H	-0.38485458	0.29513783	4.71477800
O	0.18099884	1.92783639	3.51697126
O	-1.93614219	2.83620864	0.07422978
H	3.10872438	0.09944180	4.32452314
C	2.92846162	4.14167695	-0.29421951
H	2.43863775	1.34993785	-4.21811062
O	0.56529808	1.97670828	-3.55370081
O	1.67704967	4.09252579	-0.16187952

H	-0.46708762	-1.35233240	-4.24548624
C	1.90321269	-3.21586627	-3.01274899
H	5.28730062	0.55729279	-2.05387837
O	2.17149776	-3.48314071	-1.81115104
H	5.33899249	2.49717719	1.05869223
C	0.15552852	3.08513496	-3.14092926
O	3.72974823	3.17433766	-0.32032419
O	-0.15837305	3.39278232	-1.95718581
H	5.83030141	1.01060650	1.19464613
H	3.48481528	0.82166745	-3.15545043
O	1.49132275	-2.12401732	-3.47703825
C	-0.78485058	-4.04611695	0.11177453
H	0.26088848	-1.12741583	4.83282844
O	2.08532802	-1.77022977	3.62168605
O	0.47567206	-4.00761742	0.19440185
C	-0.18308205	3.04449926	3.07714930
O	-2.93242872	0.84106392	0.36965976
O	-0.07983322	3.46824039	1.89405014
Zr	0.25041035	2.37555642	-0.02449179
O	0.38771288	-1.38177984	-0.93702685
O	2.09415313	1.86278053	1.37771752
O	-0.80702192	0.78220549	-1.37996886
O	2.52181185	-0.57696652	1.02412942
O	0.28597848	-1.66785424	1.60346877
O	-0.19463504	0.73021437	1.09589474
O	1.66736031	1.34796015	-1.10587484
O	2.80386377	-0.88066488	-1.47694852
O	-2.40980312	-1.28870444	1.87727358
Zr	-1.29258079	-0.79192082	0.21719306
O	-0.17184580	-0.51269296	4.22671169
Zr	1.29442993	0.13199017	2.52776808
O	2.64972051	0.79976572	3.85043689
O	2.73407975	0.54693497	-3.76763554
Zr	0.91031253	-0.11388727	-2.50388858
O	-0.45725310	-0.44706127	-3.91871202
O	4.53901491	1.15245274	-1.94137651
O	5.06201282	1.59395755	1.26111763
H	-0.11336590	-2.31424799	2.19405738
H	3.48807421	-1.26664267	-2.03117982
H	-1.54469978	1.03547760	-1.94392803
H	2.45731744	2.56217109	1.92956888
H	-4.68281006	-1.61734743	-0.38284277
O	-2.65321359	-1.20634586	-1.48806103
C	-3.72141703	-1.83890874	-1.67677696
O	-4.20239406	-2.45086457	-2.59841566
C	-5.17825253	-1.32787725	0.68624258
C	-6.59000415	-1.22424022	0.42434802
H	-4.70051852	-0.35529095	0.85634384
O	-4.85476256	-2.28756144	1.62952189
N	-7.13161237	-0.35768342	-0.39232337
H	-7.26033017	-1.95866382	0.86554466
H	-3.90399970	-2.10471599	1.82689433
C	-6.34131976	0.64595586	-1.12145246
C	-8.59004446	-0.32664217	-0.55787271
H	-5.28147761	0.42132966	-1.00576033
H	-6.59327741	0.55970262	-2.18124092
C	-6.60785021	2.06199688	-0.64166652
H	-8.81882526	0.24945368	-1.45604141
H	-8.95507847	-1.34488575	-0.70867921
C	-9.27524428	0.30666553	0.65212629
H	-7.65451423	2.34134922	-0.81997225
H	-5.97890667	2.73297771	-1.24079160
O	-6.28326428	2.11572790	0.73185152
H	-8.83457777	1.29138362	0.85702816
H	-9.09902765	-0.32113782	1.53754148
O	-10.64252412	0.38539091	0.32720077
H	-6.48962604	2.99546511	1.06112762

H	-11.11097930	0.74971212	1.08308075
H	2.81024863	-3.61093487	3.95983854
H	6.09497206	-2.41090408	0.27351713
H	2.05618382	-4.03145260	-3.73477555
H	-1.22999815	-5.05005998	0.04522559
H	-0.63217501	3.73960370	3.80215830
H	3.36581374	5.14613620	-0.39223339
H	-3.90492694	2.58896872	0.41760703
H	0.04404377	3.88445848	-3.88941427

4

$$\Delta G = -3120.209517$$

O	-2.29290672	-2.90294670	1.89680937
C	-1.55865547	-3.90495292	1.69142176
O	-0.40422741	-3.91326331	1.18860783
Zr	0.75907726	-2.34630889	0.10282807
Zr	-2.03420724	-0.64710523	1.47238031
C	-0.67765712	-3.79690166	-2.41517950
H	1.77420168	1.50943803	-4.03989838
O	3.38740455	-0.94047401	-1.92448084
O	0.11617030	-3.84041534	-1.44081043
C	1.13589248	3.76417687	-2.05414150
H	-1.33321577	0.08258852	-4.72070991
O	-2.24444903	1.19536090	-3.23992926
O	0.16367412	3.85960514	-1.26274330
H	-3.44121208	-2.09298130	-2.73623116
C	-3.65461248	2.20590284	1.66814491
H	0.14556277	1.17497317	4.52656443
O	0.67097009	2.61347118	3.04109719
O	-2.86836672	2.85113477	0.92589210
H	3.68959880	0.79686153	2.77360901
C	2.74175953	-2.33620497	2.61801527
H	-2.22171603	-1.54666699	3.95259179
O	2.17822120	-2.97607635	1.68662104
H	-4.85614421	-0.78913470	1.47580602
C	0.09736627	3.63580905	2.59926739
O	-3.58103056	0.99000792	1.97557393
O	-0.41898891	3.78747940	1.45784284
H	-4.32544649	-2.26731031	1.43528927
H	-0.70606933	-0.06643200	4.02885745
O	2.54403907	-1.14132907	2.94767109
C	3.49444379	-2.15287422	-1.60876502
H	-0.80949567	-1.39888579	-4.76245617
O	-1.29449259	-2.78664499	-2.84311844
O	2.66668151	-2.84368001	-0.95588193
C	-2.48911138	2.38271859	-2.91729146
O	1.84349345	2.74387546	-2.26990409
O	-2.28456774	2.92043720	-1.79474388
Zr	-0.97234847	2.31456356	-0.11109139
O	1.65614586	-0.49905596	0.31695463
O	-2.50682295	0.51681256	-0.45434571
O	1.29077153	1.97702934	0.35980321
O	-1.11811346	-1.55369041	-0.21202665
O	0.73133930	-1.23314073	-1.98038895
O	-0.19197842	0.99903159	-1.45158828
O	-0.77438324	0.93095622	1.40756454
O	0.02712671	-1.37894273	2.04274406
O	1.77784014	0.59142506	-3.73768442
Zr	1.85814908	0.64767460	-1.38319261
O	-0.72808593	-0.55153823	-4.30415476
Zr	-1.45960483	-0.63616256	-2.02687992
O	-3.33619405	-1.17854608	-2.45576197
O	0.23112590	0.28936142	4.14887529
Zr	1.23279667	0.55663189	2.09722149
O	2.97990425	1.40356125	2.54077253
O	-2.12547864	-0.68205564	3.54033748

O	-4.19717339	-1.37633640	1.08313657
H	1.10736683	-1.80207598	-2.65846757
H	0.07129132	-1.94503097	2.81927008
H	1.89899331	2.71129644	0.49821242
H	-3.42244756	0.72471638	-0.66588573
H	4.32643954	-0.08932417	0.48846657
O	3.70220943	1.42484691	-0.70408446
C	4.61571197	0.88490818	0.04963674
O	5.70843512	1.37554852	0.28168004
H	0.96838848	0.17529097	-4.09001582
H	-2.93982945	3.02396105	-3.68812576
H	-4.50054734	2.77036613	2.08571489
H	0.04262395	4.50443001	3.27173288
H	1.40120650	4.67001902	-2.61640016
H	4.40242388	-2.67138990	-1.94604370
H	-1.96373993	-4.88029101	1.99521147
H	-0.84102035	-4.74009915	-2.95484639
H	3.48112104	-2.89601509	3.20777436

4'

$\Delta G = -3043.81376$

O	-2.45094599	2.62138420	2.01942398
C	-3.56432431	2.06582142	1.81585343
O	-3.76966898	0.94541411	1.28466621
Zr	-2.44547472	-0.42436180	0.08791530
Zr	-0.29378092	1.98879325	1.54634580
C	-3.68025579	1.32428003	-2.32142825
O	-1.52619453	-3.26419851	-1.87647723
O	-3.85274302	0.52094339	-1.36691809
C	3.60316203	-1.86932838	-1.97440044
H	0.24103083	1.38631780	-4.67153164
O	1.52946251	2.08017148	-3.16540480
O	3.79587191	-0.82317596	-1.28895061
H	-1.52924926	3.75459360	-2.54444018
C	2.82625635	3.04482628	1.78308090
H	1.19105285	-0.59741130	4.45594632
O	2.39073553	-1.60526150	2.86459324
O	3.32308186	2.18668699	1.00515654
C	-2.66386527	-2.49016329	2.56617530
H	-1.12886356	2.19356595	4.04314889
O	-3.23866313	-1.79348577	1.68984899
H	0.09372942	4.77629151	1.69275696
C	3.50358194	-1.10403357	2.53092467
O	1.61643520	3.17814120	2.09304468
O	3.74838793	-0.40112465	1.52208332
H	-1.45835475	4.53697411	1.64502211
H	0.11793039	0.48294207	4.00922822
O	-1.43396709	-2.50670789	2.84059107
C	-2.73248201	-3.15496913	-1.56430416
H	-1.31963691	1.24636265	-4.67412452
O	-2.58554516	1.77899883	-2.74084822
O	-3.28206542	-2.19394849	-0.95299060
C	2.74105838	2.11310752	-2.84473908
O	2.51927805	-2.47037857	-2.15162774
O	3.24402305	1.77698502	-1.73685434
Zr	2.43582851	0.48574871	-0.11721166
O	-0.75139948	-1.55971971	0.22733715
O	0.93299055	2.30871065	-0.35633490
O	1.75609455	-1.64097921	0.24916233
O	-1.35377323	1.31659273	-0.15333661
O	-1.39036028	-0.50462711	-1.97177192
O	1.01259375	0.00970091	-1.47931603
O	1.03902923	0.45079184	1.43271405
O	-1.34860647	0.06182283	2.05185198
O	0.32401231	-1.91724915	-3.57432726
Zr	0.34555879	-1.97154018	-1.58264661

O	-0.50771173	0.93631071	-4.25264731
Zr	-0.40168772	1.53446371	-1.97309145
O	-0.63187050	3.49670284	-2.31147637
O	0.31167293	-0.50395969	4.07039507
Zr	0.33070984	-1.45773882	1.94335957
O	-0.28545279	2.01018534	3.61656851
O	-0.60925791	4.26344129	1.27278675
H	-1.96837430	-0.74169973	-2.70281735
H	-1.90027419	0.06527947	2.83963251
H	2.45420614	-2.29245894	0.35652175
H	1.30657153	3.17759643	-0.53381529
H	0.91354506	-5.42897466	0.79001715
O	0.70742072	-3.97604730	-0.57649718
C	0.76688176	-4.35341002	0.61864868
O	0.68613331	-3.63440578	1.65513394
H	-0.08649535	-1.19029993	-4.05460272
H	3.44517107	2.48803839	-3.60176928
H	3.53252128	3.75682084	2.23361018
H	4.34773204	-1.31659136	3.20196322
H	4.49417536	-2.29483734	-2.45816226
H	-3.39883118	-3.97864507	-1.85921412
H	-4.45324475	2.61800685	2.15227639
H	-4.58697202	1.65585475	-2.84715069
H	-3.30558011	-3.15082729	3.16517136

H₂TCPP-Zr₆ model used for TD-DFT calculations

C	12.04419241	4.12966725	0.25516697
H	12.01850646	5.20590585	0.33593927
C	10.90830989	3.27500479	0.40105937
C	13.89701711	-1.58765369	-0.65409923
H	14.97615383	-1.54893047	-0.63926401
C	17.11934180	1.65135369	0.27080340
H	17.77782499	1.94700774	1.08113819
C	17.63261155	1.43489516	-1.00420623
C	14.91783786	1.08497013	-0.53680995
C	15.75983427	1.47813245	0.50488186
H	15.34640301	1.63311998	1.49683711
C	16.79945426	1.05779465	-2.05194696
H	17.20660085	0.89907110	-3.04519527
C	13.00078749	-0.45894951	-0.44482833
C	13.46788193	0.85427783	-0.30480643
C	15.44243344	0.88323225	-1.81692713
H	14.77832986	0.58260819	-2.62135471
C	7.19164365	3.14332758	1.20574867
H	6.91461952	4.12137325	1.57079209
C	9.47689861	7.22276356	1.92661972
H	9.87829189	7.82343080	2.73648752
C	8.62606245	7.79746492	0.98577377
C	9.28318418	5.09307357	0.80131986
C	9.80623059	5.87368532	1.83504945
H	10.45916610	5.41722724	2.57290761
C	8.10751553	7.03033703	-0.05269516
H	7.44932582	7.47960645	-0.78932579
C	8.52023732	2.74280324	0.76974461
C	9.59006057	3.64267579	0.67794293
C	8.43583985	5.68373884	-0.14342614
H	8.03527178	5.07618010	-0.94894152
C	13.12908318	3.34170913	-0.00516796
H	14.14610280	3.66113340	-0.17548300
C	12.68863737	1.98107050	-0.03750243
N	11.34620005	1.99273197	0.21627207
C	-2.09760936	-5.64954103	3.72913122
H	-1.17766041	-5.15573150	3.43769186
C	-3.31544105	-5.15778653	3.26005666

C	-3.29855962	-7.34497810	4.92261426
C	-2.09067017	-6.75239113	4.56941256
H	-1.15589883	-7.14770283	4.95229822
C	-4.52264642	-5.76552694	3.60794994
H	-5.45096964	-5.36366450	3.21899108
C	-4.51419988	-6.86912355	4.44528770
H	-5.44187367	-7.35435517	4.72905476
O	-7.27786816	-0.86374896	1.10506291
C	-8.43354629	0.65937338	-4.40112861
H	-8.50119673	1.42491628	-3.63583359
C	-7.25131838	-0.07349941	-4.53044482
C	-9.41085819	-0.61455783	-6.20048863
C	-9.51231348	0.38674835	-5.23556245
H	-10.43431932	0.94904676	-5.12991924
C	-7.15003545	-1.06958059	-5.50557296
H	-6.22746418	-1.63267297	-5.59089882
C	-8.22739307	-1.33679646	-6.34166544
H	-8.14867790	-2.11195008	-7.09684599
C	-0.49279161	-6.08404772	-0.70117065
H	-0.16123036	-5.59651000	0.20886943
C	-1.28235961	-5.37322292	-1.60638767
C	-0.59672724	-7.99858355	-2.15222179
C	-0.15223723	-7.40253613	-0.97458616
H	0.45659158	-7.96561681	-0.27490100
C	-1.72862088	-5.97682731	-2.78381442
H	-2.33962606	-5.40496832	-3.47319217
C	-1.38181920	-7.29231015	-3.05909097
H	-1.72054943	-7.76723244	-3.97389503
C	-7.89177790	0.06891374	0.50672949
O	-7.35690385	0.95374178	-0.21308535
C	-10.11615584	1.11575338	0.09081708
H	-9.60599812	1.91909889	-0.42874781
C	-9.36793557	0.07958852	0.64947882
C	-12.11271112	0.03905722	0.87437206
C	-11.49845069	1.09545759	0.20774327
H	-12.09741044	1.89303641	-0.21872269
C	-9.99104315	-0.97578292	1.31855353
H	-9.38720593	-1.77424761	1.73292932
C	-11.37205432	-0.99696120	1.43130713
H	-11.87026555	-1.81262069	1.94423005
Zr	-5.23077863	1.37480971	-0.75173749
Zr	-5.18684783	-1.64693777	1.05997665
C	-5.51629689	3.60192987	1.55686530
H	-0.96973025	3.81123425	-0.66907392
O	-2.46997700	2.89401646	-2.34772601
O	-5.91352364	3.11296471	0.46208479
C	-6.43006191	5.82176007	0.85893052
H	-6.64577684	5.38659179	-0.11070945
C	-5.87658479	5.01817067	1.85828494
C	-6.37134795	7.70618914	2.35875509
C	-6.67349260	7.16726895	1.10956174
H	-7.09179002	7.79723674	0.33145908
C	-5.58539183	5.55974309	3.11290282
H	-5.16221760	4.92243411	3.88174007
C	-5.83739064	6.90265487	3.36416604
H	-5.61245957	7.32494520	4.33792493
H	0.34231829	1.23075538	-2.86935162
C	6.41106365	2.05090919	1.07894691
H	5.36313956	1.95310060	1.32104166
C	1.03015180	-0.37444445	-0.07441311
H	-1.59187340	2.85981866	3.52867685
O	-1.57308642	0.72473764	3.53255849
O	0.41825858	-1.30411772	0.52690605
C	3.18059343	-1.28510428	0.82058128
H	2.60327189	-1.95507649	1.44737982
C	2.51580852	-0.41546863	-0.04400001
C	5.29354031	-0.38097510	0.08989204

C	4.56709802	-1.26200411	0.89360960
H	5.08991363	-1.90909543	1.59069563
C	3.23770155	0.44975089	-0.86472906
H	2.70878242	1.11823511	-1.53345246
C	7.27104728	0.99604879	0.55699422
C	6.77136986	-0.26118025	0.17498790
C	4.61893789	0.45498649	-0.80716921
H	5.18990125	1.12566182	-1.44048033
H	-4.92988652	1.66604487	4.20878551
C	8.11826947	-3.38515007	-1.04268735
H	8.11028196	-4.38700033	-1.44483684
C	9.30159478	-2.62597890	-0.77156754
C	-3.33975357	-3.94297567	2.41391295
H	-4.52181661	-4.00951449	-2.28562151
O	-2.51596178	-3.43134610	-2.07610745
O	-2.23215671	-3.44044321	2.07655794
H	-3.17276766	-1.03011591	-4.59096435
C	-6.12450782	0.13921714	-3.57277274
H	-7.18598881	-3.03900371	0.02178780
O	-6.23664376	1.07230912	-2.72334900
H	-6.03739350	-2.71207531	3.54618728
C	7.04174329	-2.61296161	-0.71960998
H	5.99811415	-2.87322794	-0.81234102
C	7.52909871	-1.35407678	-0.23783199
C	-1.66781335	-3.96436701	-1.31278865
O	-4.47488371	-3.48191935	2.11366394
O	-1.11179319	-3.40225324	-0.32531461
H	-7.09641206	-1.63259760	3.13797174
H	-5.58324469	-3.32483599	-1.33139830
O	-5.15174774	-0.66263891	-3.63737322
C	-3.58436755	3.46549092	-2.48622645
H	-2.80926004	3.77720943	3.16290460
O	-4.78954357	2.99787135	2.39662187
O	-4.67133695	3.10254528	-1.95295147
C	-4.84071393	5.33988137	-3.52306850
H	-5.74853517	4.90293075	-3.12338427
C	-3.62088859	4.69958649	-3.30305190
C	-3.66943982	7.05267075	-4.71626473
C	-4.86460199	6.52624194	-4.23877934
H	-5.80095568	7.04270687	-4.42084771
C	-2.42686224	5.22921643	-3.79255930
H	-1.49465764	4.71258077	-3.59618982
C	-2.45147083	6.41683846	-4.50572318
H	-1.53421708	6.84973371	-4.89017797
C	13.10689150	-2.66285444	-0.85310436
H	13.40555046	-3.68507049	-1.03327286
C	10.83043421	-6.77618722	-1.34857830
H	10.59234054	-7.67062230	-0.78191252
C	11.41549549	-6.88137644	-2.60758729
C	10.87420971	-4.36700742	-1.53189135
C	10.55937079	-5.52162566	-0.81126129
H	10.11497303	-5.43141247	0.17539881
C	11.72302177	-5.73743504	-3.33769581
H	12.17227976	-5.82102398	-4.32202313
C	11.73729585	-2.18098690	-0.75643677
C	10.62444281	-3.01037226	-0.97572022
C	11.45238592	-4.48526776	-2.80077344
H	11.69053177	-3.58626489	-3.36082523
C	-0.73004402	-0.21292489	3.59705606
O	0.48774940	0.58242548	-0.68650694
O	-0.75111756	-1.26609526	2.89758679
C	1.49755222	-0.87377802	4.53986068
H	1.55025278	-1.65084065	3.78528136
C	0.37259586	-0.04906536	4.59075129
C	2.44278058	0.32218404	6.40684727
C	2.53563955	-0.68273571	5.44509546
H	3.41676177	-1.31454759	5.40151634

C	0.28371506	0.95520261	5.55811894
H	-0.60065253	1.58124987	5.59392466
C	1.31594416	1.13788911	6.46908826
H	1.24463504	1.91409410	7.22384313
H	-0.83973300	2.07453909	-3.44336893
Zr	-1.70811774	-1.65672504	0.90331679
O	-3.55347732	0.56248844	-1.58934807
O	-3.43563260	-1.04071688	2.39656072
O	-1.58361235	-0.92178159	-1.34835149
O	-4.89241148	0.44956983	1.05238019
N	8.89369189	-1.41421950	-0.28369425
O	-3.30515785	2.32858962	0.26776152
O	-1.89570566	0.36978097	0.89089699
O	-3.51113143	-1.94530236	-0.02512815
O	-5.55477861	-0.87013985	-1.02080617
O	-0.60338195	2.95298139	-0.43855047
Zr	-1.67477703	1.31373445	-0.91140663
O	-0.61192880	1.23818230	-3.01533167
O	-2.19018229	3.12231878	2.81577336
Zr	-3.38330825	1.17953616	2.23575023
O	-4.21603877	1.03777324	4.06269184
O	-5.10193217	-3.23983319	-2.21528320
Zr	-3.62805086	-1.43176367	-2.12026387
O	-2.69830517	-1.50255323	-3.89971198
O	-6.24607069	-3.20686793	0.14399583
O	-6.15085069	-1.82025095	3.19431355
N	8.55286856	1.42340067	0.42943648
N	11.69811064	-0.85311215	-0.47000854
H	-3.24872115	3.28701820	0.30817084
H	-6.39334521	-1.14591990	-1.39995869
H	-0.85900393	-1.26845293	-1.87639938
H	-3.37414763	-1.36300343	3.30052762
H	18.69543548	1.56703232	-1.18352940
H	8.36911166	8.84945389	1.06259694
H	-6.55791711	8.75815235	2.55127422
H	-3.29043915	-8.20629826	5.58467464
H	-10.25622901	-0.82945759	-6.84668411
H	-0.32741741	-9.02885456	-2.36516572
H	-13.19544529	0.02481554	0.96016017
H	-3.68857363	7.98623461	-5.27172144
H	11.62913609	-7.86161745	-3.02251574
H	3.25432379	0.46762241	7.11319159
H	9.52263419	-0.64449068	-0.08258841
H	10.73476368	1.18392376	0.19104676